Cape Peninsula University of Technology

THE EFFECT OF PARTICLE SIZE DISTRIBUTION ON THE EXTRACTION OF GOLD FROM PRINTED CIRCUIT BOARDS USING AMMONIUM THIOSULPHATE

by

Fernando Diego Morkel

A thesis submitted in fulfilment of the requirements for the degree

Master of Engineering: Chemical Engineering

in the

Faculty of Engineering and the Built Environment

at the

Cape Peninsula University of Technology

Supervisor: Dr M Aziz

March 2020

DECLARATION

I, Fernando Diego Morkel, declare that the contents of this dissertation/thesis represent my own unaided work, and that the dissertation/thesis has not previously been submitted for academic examination towards any qualification. Furthermore, it represents my own opinions and not necessarily those of the Cape Peninsula University of Technology.

F Morkel **March 2020**

Signed **Date**

ABSTRACT

The rapid advances in the fields of electronics and telecommunications have resulted in the growing generation of electronic waste (e-waste) worldwide. This waste contains hazardous heavy metals that can endanger the ecosystem. As such, environment-friendly recycling techniques are envisaged as mitigating measures. The use of hydrometallurgy to recover base and precious metals from waste computers and mobile phones has seen unprecedented attention in the past decade. Non-cyanide leaching agents such as ammonium thiosulphate show potential in the recovery of gold from waste printed circuit boards (PCBs), the central part of electronic devices.

This research project aimed to investigate the effects of particle size distribution (PSD) on the shrinking core model (SCM) for the determination of the control regime of the ammonium thiosulphate leaching of gold from waste mobile phone PCBs. The Gates-Gaudin-Schuhmann (GGS) and Rosin-Rammler (RR) models were used to describe the PSDs used. It was determined that the GGS model was a good fit for large particles (658 µm mean size) whereas the RR model was a good fit for smaller particles (503 to 433 µm mean sizes). These PSD models were used to estimate the central values (median and mean sizes) and covariances of the PSDs.

The leaching experiments were carried out in a batch setup. The PSD was varied from a mean size and median size of 658 and 592 µm to 433 and 354 µm, respectively. The pulp density was subjected to three variations: 40, 80 and 120 g/L. The other leaching conditions were fixed at levels prescribed by the existing literature. The PCBs were found to contain 172 g Au/ton-PCB based on the aqua regia characterisation. In thiosulphate leaching, almost complete gold extraction (97% in 2 hours) was obtained at 40g/L pulp density, 0.1 M thiosulphate, 0.04 M copper sulphate, pH 9.5, 30°C and 350 rpm mixing rate. These results were obtained with PCB particles with median and mean sizes of 433 and 354 µm, respectively. Reducing the pulp density from 120 to 40 g/L improved the gold dissolution from averages of 35 to 80%, irrespective of the PSD used. The variation of PSD had little to no significant impact on gold extraction at high pulp densities but did influence gold extraction at low pulp density.

The PSD covariances obtained in this study (CV < 0.3) indicated that particle size distribution could safely be excluded from the shrinking core model in determining the rate-limiting step of the leaching process. Based on the SCM, the leaching process was found to be controlled by chemical reaction and ash layer diffusion at 40 g/L pulp density. In contract, higher pulp densities hindered the shrinking of the unreacted core and corresponding gold conversion and limited the application of the shrinking-core model to describe, predict and provide insight into the rate-limiting mechanism of the leaching process. Possible reasons for the SCM not fitting the leaching data, for larger particles at low pulp density and all particle sizes at higher pulp densities, were discussed.

This research will provide insights into the overlooked particle size distribution aspect of the extraction process; assist in devising optimised mathematical models for the design of new leaching reactors; retrofitting of existing ones to include PCBs in the existing process streams and optimise the size reduction step for improved dissolution efficiency.

RESEARCH OUTPUTS

F.D. Morkel, M. Aziz, T.V. Ojumu and Y.R. Mboko; The ammonium thiosulphate leaching of gold from waste mobile phone printed circuit boards - emphasis of acid pre-treatment, CPUT Annual Post Graduate Conference, SARETEC, Cape Town, South Africa, 7 November 2018

F.D. Morkel, M. Aziz, A.A. Ismail and Y.R. Mboko; Investigate the influence of solid mass in the hydrometallurgical processing of waste mobile printed circuit boards for gold ammonium thiosulphate leaching, *International Journal of Minerals, Metallurgy and Materials*, submitted 19 February 2020 [Paper ID: IJM-02-2020-0157].

ACKNOWLEDGEMENTS

Almighty God, for giving me the opportunity to complete this research project.

I wish to thank:

- My supervisor, Dr Mujahid Aziz, for his outstanding supervision, persistent guidance, and technical expertise in the field of this research. I am gratefully indebted to him for his patience, invaluable advice, continuous support and encouragement throughout my studies.

- My co-supervisor, Prof Tunde Ojumu, for his assistance.

- Romy Mboko, for his guidance, advice and always available to assist when writing up of this manuscript.

- The technical and administrative staff in the Chemical Engineering Department, Mrs Hannelene Small, Mrs Elizma Alberts and Mr Alwyn Bester, always willing to assist.

- The Environmental Engineering Research Group (*EnvERG*) in the Chemical Engineering Department, for all their support and assistance. A special thanks to Abdul Azeez Ismail, assisting with the practical work.

- My parents, grandparents, brother, sister, family and friends, for their love, support and encouragement to complete my studies successfully.

- My wife and daughter for their continuous love and care.

- The financial assistance of the NSFAF and DAAD TUCSIN towards this research is acknowledged. Opinions expressed in this thesis and the conclusions arrived at, are those of the author, and are not necessarily to be attributed to the NSFAF.

DEDICATION

My parents and role models, for their endless love, support and inspiration;
This achievement would not have been possible without you

Thank You!

TABLE OF CONTENTS

LIST OF FIGURES

LIST OF TABLES

LIST OF ACRONYMS

AAS:	Atomic absorption spectrometry
ADC:	Ash layer diffusion control
ATE:	Advanced tropical environment
CIL:	Carbon in leach
EEE:	Electronic and electrical equipment
EPR:	Extended producer responsibilities
FDC:	Liquid film diffusion control
PCB:	Printed circuit boards
PCM:	Progressive conversion model
PPE:	Personal protective equipment
PSD:	Particle size distribution
RC:	Chemical reaction control
SCM:	Shrinking core model
WEEE:	Waste electronic and electrical equipment

LIST OF SYMBOLS

Symbol	Description	Unit
C_{Af}	Concentration of A in fluid phase	mol/m^3
$\mathcal{D}_e$	Effective diffusion coefficient of fluid reactant in ash layer	m^3/m-solid/s
df	Degrees of freedom	
k''	First-order rate constant	s^{-1}
k_f	Mass transfer coefficient between liquid and particle	m^3 liquid/m^2 surface/s
n	Sample size	
N	Number of moles	
R	Pearson correlation	
R	Particle size	µm
R^2	Coefficient of determination	
r_c	Unreacted core size	µm
t/τ	Fractional time for complete conversion	
X	Conversion	
τ	Time for complete conversion	s

CHAPTER 1

INTRODUCTION

CHAPTER 1 : INTRODUCTION

1.1 Background to Research Problem

Due to the severe abuses of resources worldwide, the extraction of gold from ores has begun to be exhausted because of the inefficient amount of raw materials readily available to supply the high demand of electric and electronic manufacturers (Birloaga et al., 2013). Globally, billions of people are using mobile phones as communication devices. Mobile phones are not only used for personal luxury but also serve as the only means of communication in certain parts of the third world (Ha et al., 2010). The constant annual generation of waste electrical and electronic equipment causes severe environmental problems as it is disposed of in landfills and because of their dangerous content.

Printed circuit boards (PCBs) are the main part in any electronic device because they ensure proper information relay from various components. As such, they contain the most considerable amount of metals such as gold, copper, and other base and precious metals (Tuncuk et al., 2012). The metallic fraction of a typical mobile phone PCB can reach as high as 50% of the entire PCB mass (Grosse et al., 2003; Hanafi et al., 2012; Chehade et al., 2012; Cui & Anderson, 2016). In fact, it has been established that the metal content of PCBs is higher than that of naturally occurring ores (Grosse et al., 2003; Montero et al., 2012; Cui & Anderson, 2016). Therefore, there are financial and environmental incentives for the recycling of gold and other metals from waste mobile phone printed circuit boards.

In South Africa, the processing of e-waste is done manually and involves steps from resorting, shredding, pulverisation and granulation, and is generally regarded as recycling. When desktop computers are processed, the computer case is preferred for upgrading and is sold as a second-hand product. The processing of e-waste does not fall under the Extended Producer Responsibility (EPR) as what is practised in European countries. The producers of electronic equipment play no role in the processing of e-waste produced except for companies who wish to boost their corporate image (ATE, 2012). Table 1-1 provides a breakdown of the E-waste processing with different companies in Gauteng.

Table 1-1: E-waste processed in Gauteng (Widmer & Lombard, 2005; ATE, 2012)

Name of a recycling company	The tonnage of e-waste recycled per year
Universal Recycling Company	2000
Mixed e-waste	2500
Printed Circuit Boards	400
African Sky	1000
Non-Ferrous Shredders cc	2000
Darkling Industrial Metal	200

Several companies make the recycling of e-waste their business, although they are not producers of e-waste. In 2005, South Africa was estimated to produce 50 000 tons of e-waste of which roughly 10% has been processed by recyclers and the rest has been dumped at general dumpsites (Anahide, 2007; ATE, 2012).

Pyrometallurgy is one of the traditional recovery techniques used in the extractive metallurgy of gold. Success has been achieved in recovering gold from electronic scraps by the Noranda process in Quebec, Canada (Veldhuizen & Sippel, 1994), and by the Boliden's Rönnskär smelter in Sweden (Lehner, 1998; Lehner, 2003). However, this recovery method is not environmentally attractive because it incurs the release of toxic gases that need to be handled with additional precautions (Khaliq et al., 2014). This process can thus be used only if appropriate equipment is used for the treatment of the evolving gases, which entails a higher capital cost for the purchase, maintenance and operation of high-performance gas emission control systems (Cui & Zhang, 2008).

Over the years, the hydrometallurgical treatment of e-waste has superseded pyrometallurgical methods because of its lower environmental footprint, ease of operation and relatively higher metal extraction efficiency (Cui & Anderson, 2016; Hanafi et al., 2012; Grosse et al., 2003). Hydrometallurgy revolves around three main operations: leaching, recovery and purification. Cyanide has been used for many years in gold leaching. However, to mitigate its adverse environmental impact, non-cyanide lixiviants such as thiourea, thiocyanate and thiosulphate are envisaged (Syed, 2012; Cui & Anderson, 2016). Thiosulphate has been praised for its higher selectivity, lower toxicity and corrosiveness (Hanafi et al., 2012; Grosse et al., 2003).

The leaching process is a series of diffusion stages between the liquid and solid phases as well as kinetic stages. As such, it relies on particle size distribution (PSD) and pulp density (PD). Many studies have investigated the effect of these parameters on various leaching processes involving naturally occurring ores (Guzman et al., 1994; Ding et al., 2013; Nosrati et al., 2014; Garg et al., 2019; Khezri et al., 2020). However, there is still a gap in the body of knowledge on the impact of incorporating the PSD and PD into the shrinking core model (SCM) to describe the thiosulphate leaching of gold from waste mobile phone printed circuit boards. Previous research established that neglecting the PSD could lead to erroneous conclusions regarding the control regime of the leaching process when the modelling is carried out with the SCM (Prosser, 1996; Gbor & Jia, 2004).

1.2 Statement of Research Problem

Mobile phone PCBs contain precious metals which can be recovered and recycled into the electronic manufacturing industry. Different treatment methods are being used to extract the metallic fraction. Thiosulphate leaching is a promising alternative hydrometallurgical treatment route to cyanidation. Many leaching processes have been characterised with the aid of the shrinking code model. However, the incorporation of particle size distribution into the SCM characterisation (modelling) of the leaching of gold from waste mobile phone PCBs is still underdeveloped.

1.3 Research Questions

Is the SCM characterisation of thiosulphate leaching sensitive to changes in particle size distribution? What effects do particle size distribution and pulp density have on the overall extraction efficiency and control regime of the leaching process?

1.4 Research Aim and Objectives

This research project aimed to investigate the effects of particle size distribution on the SCM characterisation of the ammonium thiosulphate leaching of gold from waste mobile phone PCBs.

The main objectives were:

- To identify a suitable mathematical model to describe particle size distribution.
- To determine the central values and covariances of the particle size distributions used.
- To identify the rate-limiting mechanism of the leaching process with the aid of the shrinking-core model, accounting for the PSD.
- To establish the influence of PSD and PD on the overall extraction efficiency of the leaching process.

1.5 Research Hypothesis

The PSD greatly influences the diffusion stages between the thiosulphate lixiviant and PCB particles, and in turn, the SCM characterisation of the leaching process.

1.6 Scope of this Study

Ammonium thiosulphate was used as a leaching agent in a batch reaction and copper sulphate as the oxidant. Four particle size distributions and three pulp density levels were used.

The following factors were not accounted for:

- Porosity of PCB particles
- PCB pre-treatment
- Variation in reagent concentrations, temperature, and pH
- Factor interactions between particle size distribution, pulp density and other leaching parameters such as reagent concentrations, temperature, and pH
- Leaching mechanism confirmation by activation energy determination.

1.7 Thesis Outline

Chapter 1 provides a detailed background of the entire study, calls attention to critical points of this research such as the objectives, research question and significance of the study

Chapter 2 gives an in-depth detail of literature and theory on the different topics linked to this research; the literature explores the chemistry of precious metal leaching of PCBs

Chapter 3 gives details of the materials, procedures, equipment and apparatus used for data attainment

Chapter 4 discusses the results obtained from experimental runs

Chapter 5 concludes the research based on the results achieved and gives recommendations

CHAPTER 2

LITERATURE REVIEW

CHAPTER 2 : LITERATURE REVIEW

2.1 Electronic Waste

Electrical and electronic equipment (EEE) has developed rapidly, and their average lifespans have reduced due to the changes in functions and designs. This tendency caused a large amount of waste and has become a severe environmental problem (Camelino et al., 2015). Electronic waste (e-waste) is a generic term embracing various forms of electric and electronic equipment that have stopped to be of any value to their owners. In some cases, these electronics are no longer capable of performing their intended functions efficiently while, in others, they have reached the end of their life cycle. Examples of such items include personal computers (PC), monitors, mobile phones, household appliances and entertainment devices (Akcil et al., 2015; Cui & Anderson, 2016).

Waste of electrical and electronic equipment (WEEE) has been growing due to rapid economic growth and technological advances all over the world (Kim et al., 2018). Robinson (2009) stated that e-waste is chemically and physically dissimilar from other municipal and industrial waste as it contains precious as well as hazardous and toxic materials. It requires special management and unique processing to avoid environmental pollution and potentially adverse health effects to human and animal life.

The product life cycle, especially for electronic products, has reduced significantly in recent years due to rapid advances in technology. In particular, the rapid growth in information technology and telecommunications has led to an improvement in the capacity of computers but simultaneously to a decrease in the products lifetime. This situation results in an increasing number of obsolete products that cause environmental concerns due to the rapid depletion of waste disposal capacity. The typical lifespan for a mobile phone is two years (Widmer & Lombard, 2005; Lu & Xu, 2016).

Puckett & Smith (2002) concur that when e-waste is disposed of or recycled without any controls; there are likely negative impacts on the environment and human health. E-waste contains more than 1000 different substances, many of which are toxic, such as lead, mercury, arsenic, cadmium, selenium, hexavalent chromium, and flame retardants that create dioxins emissions when burned. About 60% of the heavy metals such as mercury and cadmium found in landfills come from electronic waste. Consumer electronics make up an astonishing 40% of the lead in landfills. These toxins can cause brain damage, allergic reactions and cancer.

E-waste contains considerable quantities of valuable materials such as precious metals. First-generation PCs used to contain up to 4 grams of gold each; however, this has decreased to about 1 gram today. The value of ordinary metals contained in e-waste is also very high: 1 ton of e-waste contains up to 0.2 tons of copper (Babu et al., 2007).

According to Ongondo et al. (2011), waste electrical and electronic equipment (WEEE) is diverse. It thus becomes difficult to provide a generalised material composition for all types of waste products. Figure 2-1 shows this diversity.

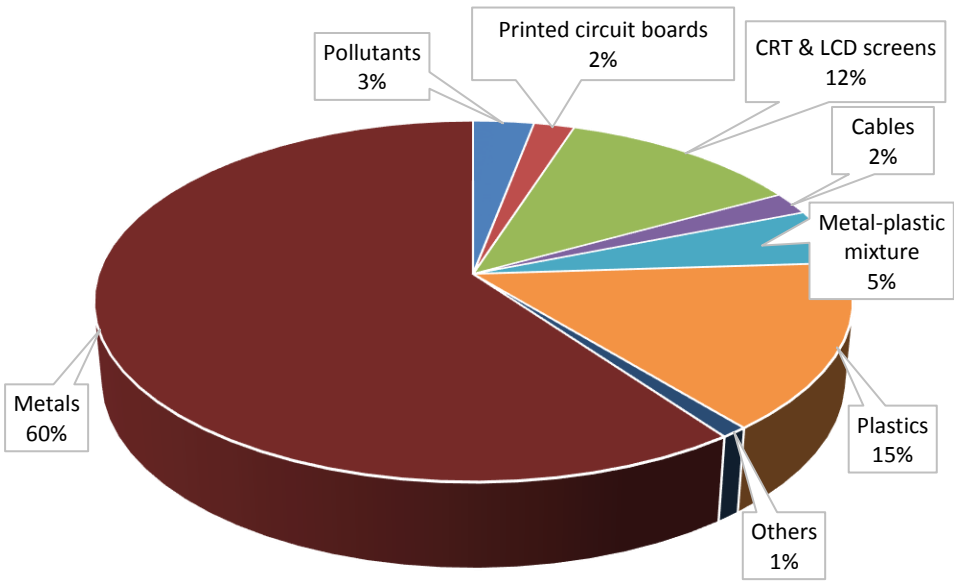

Figure 2-1: WEEE composition (Ongondo et al., 2011)

Most studies scrutinise five groups of materials, i.e. ferrous metals, non-ferrous metals, glass, plastics and other materials. Iron and steel are the most common materials found by weight, followed by plastics (Ongondo et al., 2011). Figure 2-2 shows the material composition.

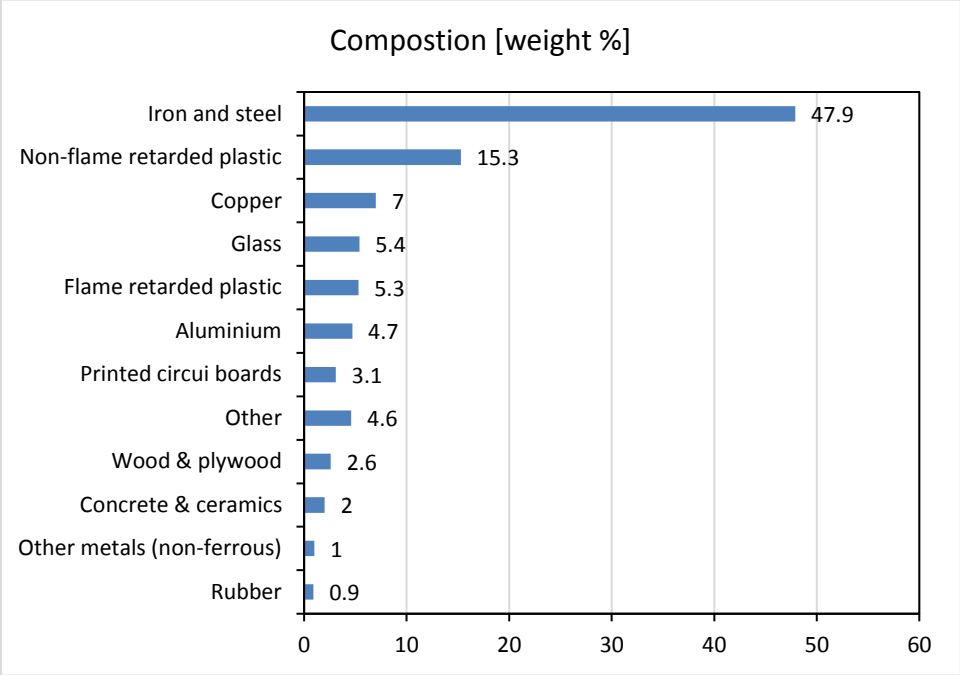

Figure 2-2: WEEE material composition (Ongondo et al., 2011)

A study conducted in 2006 estimated that the world's production of e-waste was between 20-50 million tons per annum which represented 1-3% of the global municipal waste production of 1636 million tons per annum. Computers, mobile phones and televisions, contributed approximately 5.5 million tons to the annual e-waste in 2010 (Robinson, 2009). Baldé et al. (2015) reported a worldwide e-waste production of 41.8 million tonnes in 2014, with a projected 5% annual increase. According to Lawhon (2013), in the global south, countries such as South Africa, e-waste generation was expected to triple from 2006 to 2010 and may exceed the generation of the global north by 2018.

Most of the e-waste currently processed in South Africa reportedly comes from use within the country. Recycling is usually conducted by businesses that are very selective about choosing electronics which contain the most valuable components and materials. The informal sector makes up a large part of the e-waste recycling industry. South Africa receives most electrical and electronic goods through direct purchase or second-hand purchase from various international countries outside of Africa, mainly from the global north.

South Africa also receives e-waste imports from other parts of Africa because of its high processing standards, where greater profits can be made (Lawhon, 2013). Lawhon (2013) stated that there is no explicit policy on e-waste in South Africa. However, this does not mean that the country has no legislation referring to hazardous substances or waste, or the management and disposal thereof.

In 2008, the National Environmental Management: Waste Act was introduced, which mandated the application of the waste hierarchy. The hierarchy is as follows: avoid, reduce, reuse, recycle, and then safely dispose of waste. These acts do not mention e-waste; however, the National Waste Management Strategy developed to enable provisions of the Act, which required the development of an industrial waste management plan (Lawhon, 2013).

The recycling of e-waste results in the recovery from PCBs of precious metals, such as gold; silver; copper and palladium which constitute is a substantial economic driver for developing countries (Shinkuma & Huong, 2009).

According to Tripathi et al. (2012), electronic waste is a growing concern as more and more obsolete electronic devices are discarded each year. In an attempt to reduce the impact, the waste has on the environment, is to recycle metals contained within these devices. Leaching is a hydrometallurgical liquid-solid operation used to recover metals from ores (Gupta, 2003). It is a preferable choice in many metal recovery processes as it can process ores with grade values as low as 5g/t. The use of leaching to recover metals from PCBs has become of great interest as the hazard in using leaching is much lower than that of the pyrometallurgical approach (Cui & Zhang, 2008).

2.1.1 Mobile Phone Printed Circuit Boards (PCBs)

Veit et al. (2006) state that printed circuit boards of mobile phones and computers are different in that computer PCBs are not multiplayer. Copper is found between the layers of resin in the mobile phone PCBs, and a gold layer (Au-Ni alloy) covers the conductive part of the PCBs. Thus, mobile phones contain higher concentrations of valuable minerals because of the multi-layered structures.

Figure 2-3: A typical printed circuit board (Veit et al., 2006)

A mobile phone device consists of a polymeric fraction, a printed circuit board (PCB), crystal liquid display (LCD), battery, keyboard, and an antenna (Kasper et al., 2011).

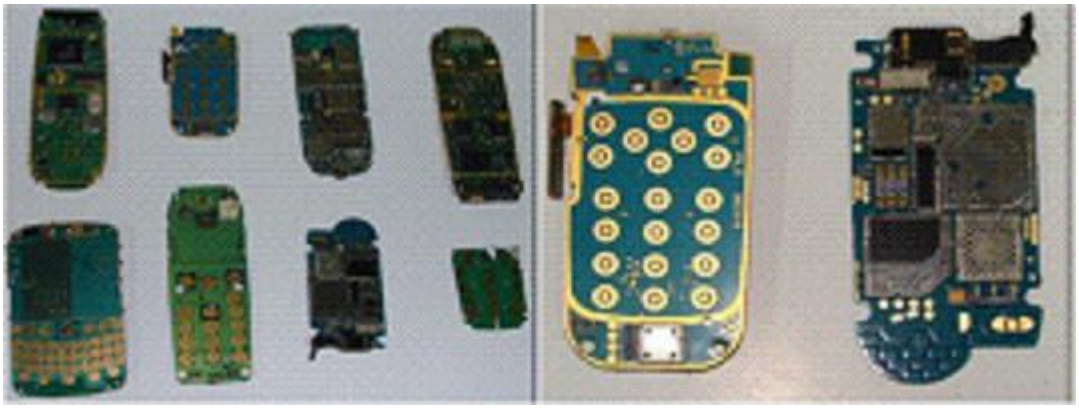

Figure 2-4: Mobile phone printed circuit boards (Osibanjo & Nnorom, 2008)

According to Schluep et al. (2009), mobile phones PCBs are made of polymers, ceramics, and metals. The metallic fraction consists of several metals, such as copper, tin, zinc, nickel, gold, silver, and palladium. The natural sources of these precious metals are limited. Their recovery and reuse are essential to augment the high demand for raw materials. From an economic perspective, the recycling of mobile phones is attractive because each ton has 130 kg of Cu, 3.5 kg of Ag, 0.34 kg of Au, and 0.14 kg of Pd on an average.

2.1.2 Characterisation of Mobile Phone PCBs

Zulkifli et al. (2016) outlined the weight components of a mobile phone PCB, as shown in Table 2-1. A typical PCB composition consists of 30% plastics, 30% refractory oxides and 40% metals. The most abundant metal is copper with a concentration ranging between 10% and 40%. The metallic content of PCBs will vary depending on the manufacturer, year of manufacturing and existing technology (Montero et al., 2012).

Table 2-1: The weight of mobile phone components (Zulkifli et al., 2016)

Type	Weight (g)
Printed circuit board	14.9
batteries	21.2
Liquid crystal display	9.3
others	44
Total	89.4

Table 2-2: The general weight composition (wt. %) of mobile phone PCBs

Au	Ag	Pd	Cu	Fe	Al	Ni	Pb	Sn	References
0.02	0.10	0.01	56.68	0.24	-	-	-	1.40	(Tripathi et al., 2012)
0.14	0.23	0.01	42.80	4.60	-	0.60	0.06	2.60	(Kim et al., 2013)
0.0347	0.363	0.0151	24.69	0.22	-	0.11	0.63	2.31	(Szałatkiewicz, 2014)
0.13	0.16	-	20.19	7.33	5.7	0.43	5.53	8.83	(Akcil et al., 2015)
0.01	0.11	0.01	40.80	0.28	-	0.39	1.36	1.60	(Xiu et al., 2015)
0.10	0.13	0.01	47.90	0.50	-	0.80	-	2.00	(Park & Kim, 2019)

According to Szałatkiewicz (2014), the Au concentration averages 0.0347 % in mobile phones which is almost twice higher than in PCB from personal computers. Furthermore, the energy required to process the waste of mobile phones equates to 7.43 MJ/kg which is lower than the chemical energy available in the waste (10.65 MJ/kg).

2.2 General E-Waste Processing Scheme

E-waste treatment is carried out in three main steps (Figure 2-5): (i) *dismantling*: to remove components such as resistors, transistors and capacitors, (ii) *pre-treatment or beneficiation*: to eliminate or reduce significantly the non-metals through mechanical-physical separation stages in order to obtain a metal-enriched solid, and (iii) *refining or end treatment*: to extract and purify the metal of interest by chemical (metallurgical) methods (Cui & Forssberg, 2003; Khaliq et al., 2014; Lu & Xu, 2016).

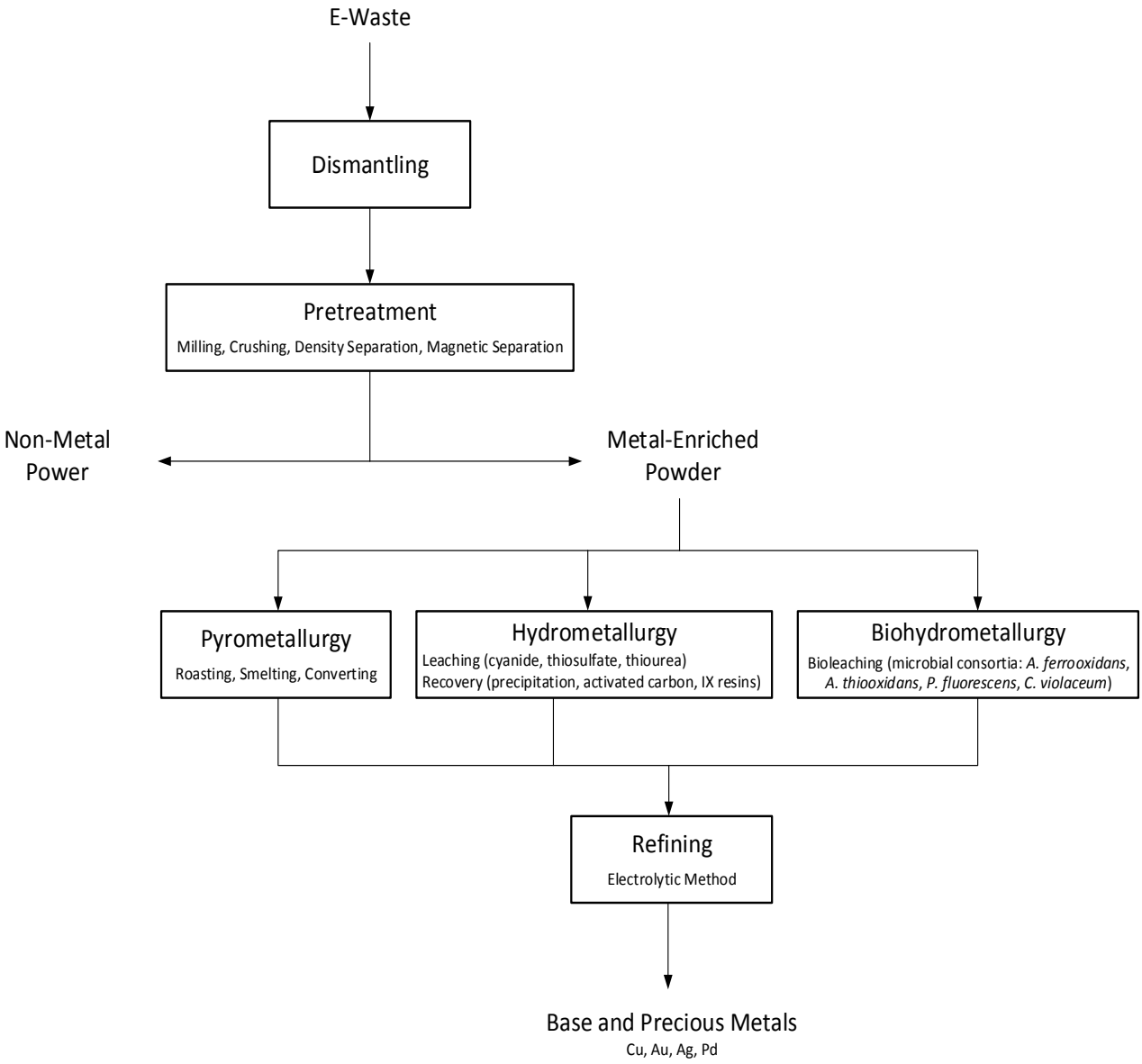

Figure 2-5: General e-waste processing scheme (Hanafi et al., 2012; Syed, 2012; Lu & Xu, 2016)

The pre-treatment or beneficiation stage is crucial because it allows the PCB particles to be freed from the unwanted non-metallic fraction. It is carried out through mechanical-physical separation stages based on physical, magnetic and electrical characteristics of the PCB constituents (J. Guo et al., 2015; X. Guo et al., 2015). Figure 2-6 shows a typical beneficiation process for e-waste treatment. This process is currently used at Shanghai Xinjinqiao Environmental Company Ltd. and Yangzhou Ningda Precious Metal Company Ltd., with a throughput of 5000 tons of waste PCBs per year (Wang & Xu, 2015).

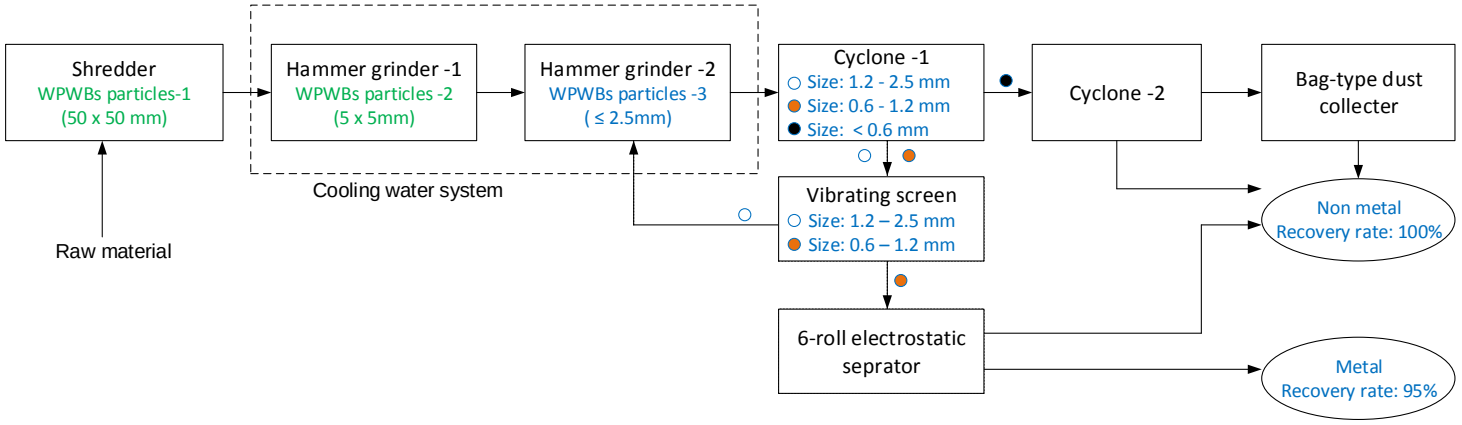

Figure 2-6: A typical beneficiation scheme for e-waste treatment (Wang & Xu, 2015)

2.3 Metal Extraction by Pyrometallurgy

Pyrometallurgical processing, including incineration, smelting in a plasma arc furnace or blast furnace, drossing, sintering, melting and reactions in a gas phase at high temperatures has become one of the conventional techniques for the recovery of non-ferrous and precious metals from secondary sources such as spent electronic scraps for the past three decades (Gupta, 2003; Cui & Zhang, 2008; Syed, 2012). The process involves the combustion of crushed waste in a furnace or in a molten batch to separate metals from non-metals, and results in the mixing of refractory oxides with metal oxide in the form of a slag phase (Gupta, 2003).

The Noranda process in Quebec, Canada was reported by Veldhuizen & Sippel (1994), and is depicted in Figure 2-7. This process treats roughly 100 000 tonnes of e-waste per year, which account for 14% of the total quantity of materials processed by this smelting system, with the major part of the feed mainly consisting of mined copper concentrates. The reactor is fed with materials

which are incorporated into the molten metal bath (1250°C) injected with oxygen-enriched air (up to 39% O_2).

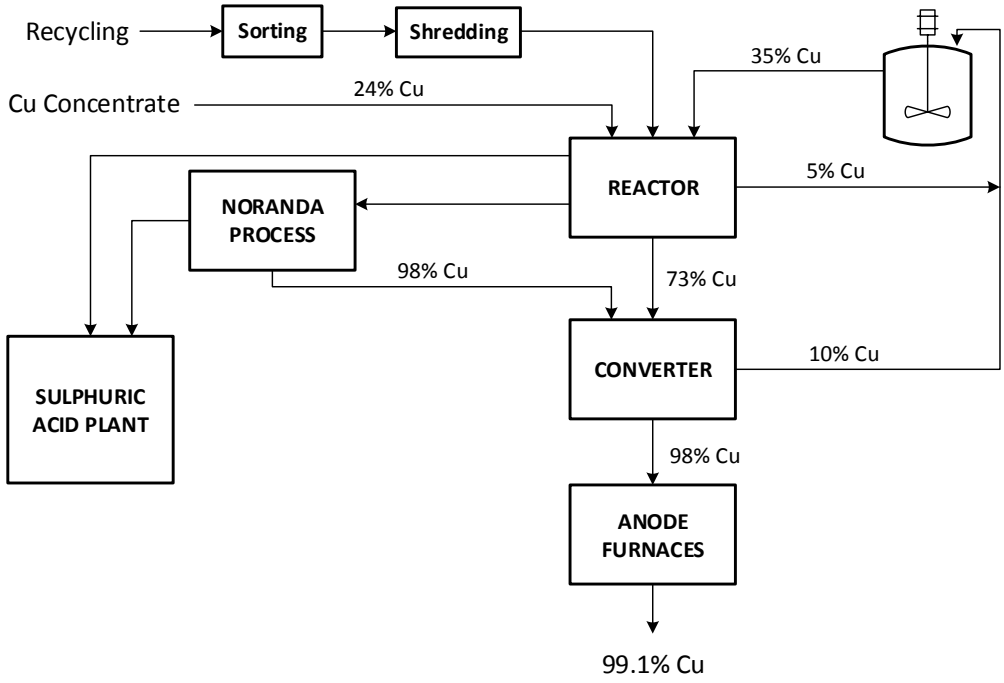

Figure 2-7: The Noranda smelting process (Veldhuizen & Sippel, 1994; Biswas & Davenport, 1994)

Another development of e-waste treatment by the pyrometallurgical route was achieved at the Boliden's Rönnskär smelter, Sweden (Lehner, 1998; Lehner, 2003). In this process, as illustrated in Figure 2-8, the location of the feed is varied based on its level of purity. The feed to the copper smelter encompasses domestic concentrates, imported concentrates, and spent secondary scraps. The feed to the lead smelter mostly consists of domestic concentrates. High-grade scrap is sent to the converting process immediately, and low-grade scrap is sent to the Kaldo furnace, which processes 100 000 tonnes of e-waste per annum (Mark & Lehner, 2000). The Kaldo reactor, a top-blown rotary converter system, uses an oxygen-oil burner in a water-cooled lance for processing e-waste mixed with lead concentrates in the feed blend. After combustion, the off-gases are further exposed to superheated air (at 1200°C).

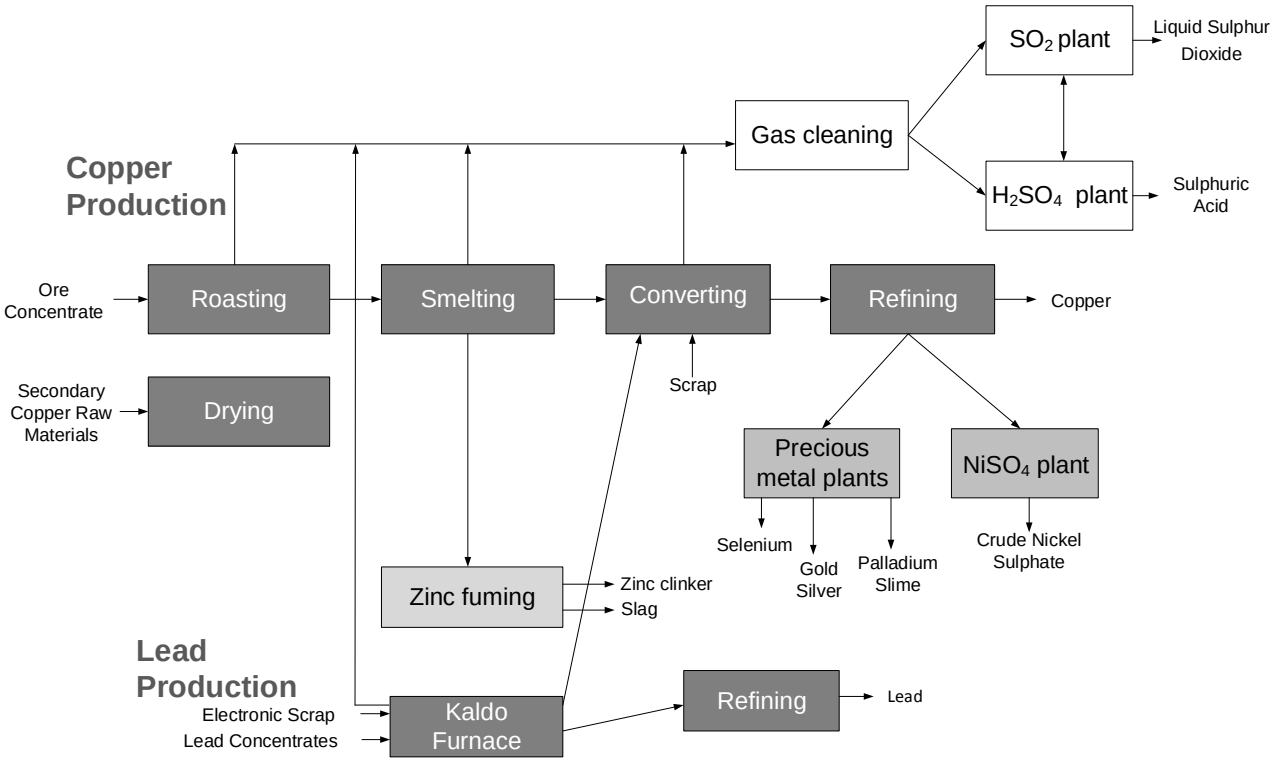

Figure 2-8: The Rönnskär smelter (Mark & Lehner, 2000)

The application of pyrometallurgy to recover metals from e-waste is still limited in the following aspects (Sum, 1991; Shuey & Taylor, 2005; Antrekowitsch et al., 2006; Ecroignard, 2006; Hageluken, 2006; Chiang et al., 2007; Dalrymple et al., 2007; Khaliq et al., 2014):

(i) Aluminium cannot be recovered by smelters, and it is known to impart undesirable properties to the slag when incorporating it.

(ii) The potential release of toxic dioxins and furans emanating from the combustion of brominated flame retardants present in printed circuit boards. Therefore, appropriate procedures are required to handle these toxic products.

(iii) The potential loss of precious and base metals to the slag caused by the presence of ceramic components in the e-waste.

(iv) Incomplete metal segregation is achievable at present, which makes the pyrometallurgical technique best suited as a pre-treatment operation.

2.4 Metal Extraction by Hydrometallurgy

Muir & Aylmore (2004) describe hydrometallurgical processes as the production of metals or metallic compounds from ores, concentrates or other intermediate materials by a sequence of operations carried out in aqueous solutions.

The main objective of any hydrometallurgical process is to extract the valuable metal from the ore through a cost-effective method. According to Aylmore (2016), any process will have one of the following technical objectives as its main:

- To produce a metal directly from ore, concentrate or pre-treated concentrate
- To produce a pure metal or metal compound from a crude metal or metal compound
- To minimise the use of water and energy in the production of metals
- To have a minimal impact on the environment in terms of the disposal of solid and liquid waste.

2.4.1 Aqua Regia

Aqua regia is one of the oldest leaching reagents used in the extraction of precious metals (Sheng & Etsell, 2007). It is still currently used as a metal characterisation method because of its ability to digest most base and precious metals (Vats & Singh, 2015). It is a mixture of nitric acid and hydrochloric acid in a molar ratio of 1:3. Metal digestion in aqua regia proceeds according to the following reactions:

$$2HNO_3 + 6HCl \longrightarrow 2NO + 4H_2O + 3Cl_2 \quad (1)$$

$$2Au + 9HCl + 3HNO_3 \longrightarrow 2AuCl_3 + 3NOCl + 6H_2O \quad (2)$$

$$3HCl + HNO_3 \longrightarrow Cl_2 + NOCl + 2H_2O \quad (3)$$

When aqua regia is diluted in water, the nitrosyl chloride formed through equations (2) and (3) recombines with chlorine to produce hydrochloric acid and nitric acid by reversing reaction (3) (Sheng & Etsell, 2007).

2.4.2 Cyanide Leaching

Cyanide has been utilised as a lixiviant for gold in the mining industries for more than one century (Hilson & Monhemius, 2006). However, various studies have reported its adverse effects on the environment due to the significant amount of cyanide-containing wastewater produced (Zhang et al., 2012). Furthermore, several cyanide-driven incidents have been reported with major detrimental effects on rivers and plants (MiningWatch, 2006; Guerra, 2010; Holland, 2015).

Aylmore & Muir (2001) stated that metal cyanide species such as copper cyanide ends up in the dam tailings. Residential areas are moving closer to these contaminated water table areas due to population growth and create a health and safety challenge.

The mechanism of gold dissolution in cyanide solution is essentially an electrochemical process. The overall reactions are shown in reactions (4) and (5) (Dorin & Woods, 1991).

$$4Au + 8CN^- \longrightarrow 4Au(CN)^{2-} + 4e \quad (4)$$

$$O_2 + 2H_2O + 4e \longrightarrow 4OH^- \quad (5)$$

Dorin & Woods (1991) investigated the effect of pH on the dissolution rate for the noble metals (gold, silver, palladium, and platinum). The results showed that a maximum dissolution of gold, silver, palladium, and platinum in cyanide solution could be obtained at pH 10–10.5. The order of activity for noble metals is Au > Ag > Pd > Pt.

Due to the various environmental concerns about the use of cyanide, several substitutes have been proposed. In general, the non-cyanide lixiviants thiourea and thiosulphate are regarded as being the most realistic substitutes.

2.4.3 Halide Leaching

According to La Brooy et al. (1994), the use of halide systems for gold dissolution predates cyanidation. Except for fluorine and astatine, all halogens have been tested and used for the extraction of gold (Hilson & Monhemius, 2006). Dönmez et al. (2001) indicated that gold forms both Au (I) and Au (III) complexes with chloride, bromide and iodide depending on the solution

chemistry conditions. However, of the halides, only chlorine/chloride has been applied industrially on a significant scale.

Sheng & Etsell (2007) stated that chlorination rates are favoured by low pH, high chloride and chlorine levels, increased temperatures, and high surface areas. According to Cui & Zhang (2008), several investigations have been undertaken to determine the effectiveness of chlorine as a leaching reagent for gold extraction. However, the industrial application of chlorine leaching is more complicated than that of cyanide leaching for two main reasons:

- Special stainless steel and rubber-lined equipment is required to resist the highly corrosive acidic and oxidising conditions;
- Chlorine gas is highly poisonous.

2.4.4 Thiourea Leaching

The usage of thiourea ($(NH_2)_2CS$) as a gold leaching agent has shown considerable promise to recover gold from ores (Veglio et al., 2003). Thiourea dissolves gold in acidic conditions, forming a cationic complex; the reaction is rapid, and gold extractions of up to 90% can be achieved (Hilson & Monhemius, 2006). The anodic reaction proceeds as follows (Niu & Li, 2007):

$$Au + 2CS(NH_2)_2 \longrightarrow Au(CS(NH_2)_2)_2^{+} + e \quad (6)$$

Pyper & Hendrix (1981) reported the following considerations on gold thioureation:

- The rate of leaching is contingent upon thiourea and oxidant concentrations;
- The use of ferric ion in sulphuric acid is the most effective system;
- The ferric ion ties up thiourea in iron-thiourea complexes; and
- The rate of gold dissolution is strongly determined by pH.

A comparison of cyanidation and thiourea leaching process in gold recovery from refractory ore was investigated by Gönen et al. (2007). They stated that only 75% extraction was achieved at very high thiourea and ferric sulphate consumptions, thus very expensive. For this reason, the direct application of the carbon-in-leach (CIL) process in gold recovery from refractory ores, as well as direct cyanidation method, are not adequate.

Despite the proven effectiveness of thiourea as a gold leach reagent, there still few full-scaled operations in existence. Its commercial application has been hindered by the following three factors (La Brooy et al., 1994):

- It is more expensive than cyanide;
- Its consumption in gold processing is high because thiourea is readily oxidised in solution;
- The gold recovery step requires continued development.

2.4.5 Thiosulphate Leaching

Thiosulphate ($S_2O_3^{2-}$), a chemical used widely in photography and the pharmaceutical industry, has also been proposed as a substitute for cyanidation by many researchers (Grosse et al., 2003; Cui & Zhang, 2008; Syed, 2012; Zhang et al., 2012). Furthermore, Muir & Aylmore, (2004) state that the main chemical components of the leaching process such as ammonium thiosulphate and ammonium sulphate are conventional fertilisers, which can be used in the agriculture industry in the production of fertiliser products.

The thiosulphate leaching of gold ores has a greater potential to reduce the impact on the environment compared to the cyanidation leaching. Unlike cyanide, which is highly toxic, the chemicals used in the thiosulphate leaching process are non-threatening, and there is a significant potential to apply the technology in those jurisdictions of the world where the use of cyanide is banned outright or is subject to intense negative publicity for environmental reasons (Akcil et al., 2015; Cui & Anderson, 2016). Similarly, Isildar et al. (2017) confirmed that precious metal leaching with thiosulphate is a non-toxic alternative to cyanidation for primary ores and secondary raw materials. Gold leaching rates can be faster than cyanidation with lower interference from other cations, thus improving the yield. Liang et al. (2013) suggested that full-scale thiosulphate leaching operation can be more cost-effective than cyanidation.

The chemical properties of thiosulphate include:

- The tendency to be oxidised;
- The tendency to hydrolyse at pH < 5.5 to S^0 and HSO_3 at mildly acid pH (Skoog et al., 2013) and more complex mixtures in strong acid (Smith & Hitchen, 1976);
- Moderately good hydrolytic stability in basic solutions (Pryor, 1960);

- Ability to form complexes with a variety of metals, e.g. gold, silver, copper (Cu+ and Cu2+) and iron (Fe3+), with the stability of these complexes depending on the solution conditions (Burns et al., 1981);
- Formation of metal sulphides, e.g. with copper, silver, mercury. Stability towards reduction to free sulphide (Burns et al., 1981).

An in-depth review of the thiosulphate leaching process applied to e-waste is provided in section 2.5.

2.4.6 Metal Extraction by Biohydrometallurgy

Bioleaching has been used successfully with copper sulphides and as a pre-treatment method for refractory gold ores. It is also used in the extraction of other base metals such nickel and zinc (Rohwerder et al., 2003). Recent studies have been focused on the utilisation of acidophilic bacteria to treat e-waste, extract metals from oxidised ores, and selectively retrieve metals from process waters and waste streams (Johnson, 2014). Bioleaching is praised for the following aspects: (i) less expensive and more flexible operability, and (ii) ability to extract metals from low-grade ores and wastes.

The mobilisation of base and precious metals in e-waste has been achieved by a number of microbes, including chemolithotrophic, heterotrophic and thermophilic bacteria (Brandl et al., 2001; Ilyas et al., 2007; Xiang et al., 2010; Chi et al., 2011). However, many of the investigations in this field have been directed towards copper and gold as metals of interest (Baniasadi et al., 2019). Chemolithotrophic (mesophilic) and heterotrophic cyanogenic bacteria are targeting the mobilisation of copper and gold, respectively (Arshadi & Mousavi, 2015; Li et al., 2015; Işıldar et al., 2016). It is noteworthy that the use of cyanogenic bacteria for gold extraction involves the production of less hazardous cyanide which has been detoxified by these bacteria to form β-cyanoalanine through β-cyanoalanine synthase (Natarajan, 2018). Recent research have shown success in incorporating microorganisms into conventional leaching systems for further improvement of gold extraction from waste PCBs (Rizki et al., 2019).

The use of biohydrometallurgy for the treatment of e-waste is still prone to several issues including the toxic nature of the waste, and precipitation of the metal of interest because of jarosite formation. The toxicity of the waste is associated with the heavy metals that can have an adverse impact on microbial growth (Ruan et al., 2014; Baniasadi et al., 2019). Furthermore, the non-

metals (plastics and brominated flame retardants) cannot be digested by microbes and can be harmful to these organisms at certain concentrations (Valix, 2017). Future developments in this field should target cyanide-degrading microorganisms, metal recovery from bio-leachates as well as the genetics of the microorganisms involved to further the understanding of the metal solubilisation process, and envisage controlled genetic mutations for improved microbial digestion and leaching kinetics.

2.4.7 Comparison of Current Leaching Technologies

Figure 2-9 indicates possible gold dissolution by using non-cyanide lixiviants. The use of thiosulphate is promising by virtue of its wider stability region compared with the other alternative leachants. However, the stability regions of these reagents are narrower than that of cyanide, i.e. high oxidising potentials can result in increased reagent consumption, hence the need for proper control of the leaching conditions.

Table 2-3: Comparison of lixiviants used in gold extraction from e-waste (Quinet et al., 2005; Zhang et al., 2012; Akcil et al., 2015; Cui & Anderson, 2016)

Lixiviant	Gold Extraction	Reagent Cost	Corrosive	Toxicity	Research Level	Extent of Commercialization
Cyanide	High	Low	None	High	Extensive	Fully established for ores
Thiourea	Average	High	Low	Low	Extensive	Limited to Ores
Thiocyanate	Low	Moderate	Low	Moderate	Low	None reported
Chloride	High	Moderate	High	Moderate	Low	Electrolytic copper slimes
Bromine	High	High	High	Moderate	Low	None reported
Iodide	Above average	High	Moderate	Low	Low	None reported
Thiosulphate	Above average	Moderate	None	Low	Extensive	Semi-commercial

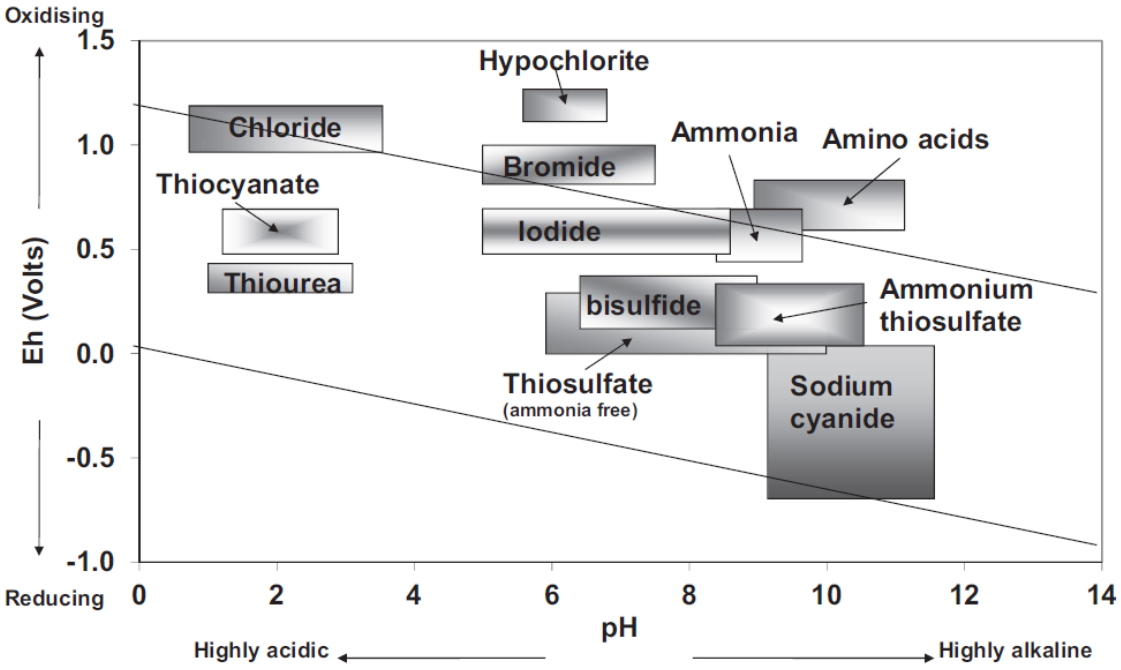

Figure 2-9: Stability regions of lixiviants used in gold extraction (Aylmore, 2016)

2.5 Ammonium Thiosulphate Leaching of Gold from E-waste

2.5.1 Leaching Mechanism

It is understood that gold dissolution in ammoniacal thiosulphate solution is an electrochemical reaction catalysed by the presence of cupric ions. The electrochemical-catalytic mechanism of gold leaching by ammoniacal thiosulphate was investigated by Aylmore & Muir (2001). It was proposed that the $Cu(NH_3)_4{}^{2+}$ species present in solution acquires electrons on the cathodic portion of the gold surface and is directly reduced to $Cu(S_2O_3)_3^{5-}$. At the same time, either ammonia reacts with Au^+ ions on the anodic surface of gold to produce $Au(NH_3)_2^+$ which, in turn, is converted to $Au(S_2O_3)_2^{3-}$ by reacting with thiosulphate ions. The $Cu(S_2O_3)_3^{5-}$ species is converted back to $Cu(NH_3)_4{}^{2+}$ with oxygen, thus achieving the regeneration of the copper amine complex. The predominant cathodic reaction will depend on the relative concentrations of the species in solution. Figure 2-10 is a depiction of the leaching mechanism with gold oxidised to the gold thiosulphate complex on the anodic side, and copper reduction on the cathodic side.

The role of Cu(II) ions in the oxidation of metallic gold to aurous Au^{+} ion can be simplified as:

$$Au + [Cu(NH_3)_4]^{2+} + 5S_2O_3^{2-} \longrightarrow [Au(S_2O_3)_2]^{3-} + [Cu(S_2O_3)_3]^{5-} + 4NH_3 \quad (7)$$

$$4[Cu(S_2O_3)_3]^{5-} + 16NH_3 + O_2 + 2H_2O \longrightarrow 4[Cu(NH_3)_4]^{2+} + 12S_2O_3^{2-} + 4OH^{-} \quad (8)$$

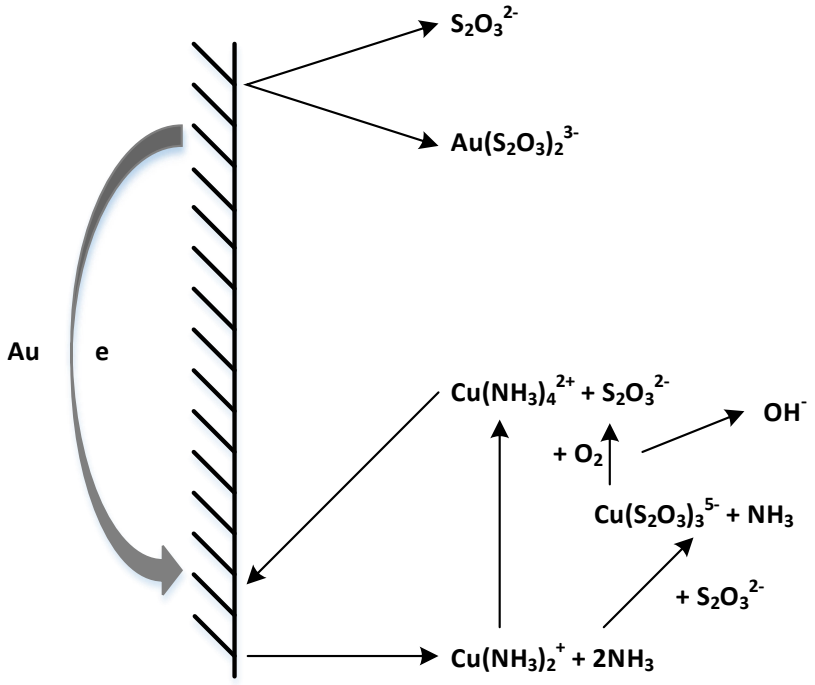

Figure 2-10: Electrochemical-catalytic mechanism model for gold leaching with ammonium thiosulphate (adapted from Aylmore & Muir, 2001)

According to Isildar et al., (2017), the presence of ammonium ions and cupric ions in the leaching system promotes the complexation of precious metals such as gold and silver. It allows the solubilisation of gold as a stable anionic complex in alkaline or near-neutral solutions. Cupric ion acts as a catalyst in the dissolution reaction, and NH_4^+ as a stabilising agent of the system and thereby accelerate the anodic dissolution.

According to Molleman & Dreisinger (2002), the chemistry of the ammoniacal thiosulphate system for gold recovery involves many interrelated chemical equilibria which are not yet fully understood. This complexity can be attributed to the presence of the three essential components involved in the leaching system, namely ammonia, thiosulphate and copper (Aylmore, 2016). Many side reactions can occur between these species, dissolved metal ions, atmospheric gases and ore minerals. Another complication of the system is that thiosulphate is prone to oxidative degradation,

thiosulphate is a metastable sulphur species which will eventually decompose in aqueous solutions (Grosse et al., 2003). Hence the need for careful monitoring and control of the operating conditions governing the ammonium thiosulphate leaching of gold.

Molleman & Dreisinger (2002) mentioned that the leaching process should not be carried out over extended periods as the degradation of thiosulphate can occur and, in the presence of copper ions, can cause the precipitation of copper sulphide, thus inhibiting gold recovery by surface passivation. Previous studies have reported that this leaching process is strictly dependent on the pH in the range of 9-10, and operating at ambient temperature to further improve the thermodynamic stability of the Cu(II)-ammonia-thiosulphate system (Perez & Galaviz, 1987; Zipperian et al., 1988; Molleman & Dreisinger, 2002). Furthermore, low cupric amine concentrations are favourable since higher concentrations are known to accelerate thiosulphate degradation (Wang, 1992; Marchbank et al., 1996; Molleman & Dreisinger, 2002).

2.5.2 Factors Influencing the Ammonium Thiosulphate Leaching of Gold

2.5.2.1 Thermodynamics

According to Breuer & Jeffrey (2002), thiosulphate leaching is a corrosion reaction. Therefore, it is possible to study the system using standard electrochemical techniques. During the gold oxidation, the leaching solution needs to include thiosulphate, ammonia and copper(II). The oxidation of gold is dependent on the solution chemistry generated by the addition of copper(II) to the solution.

Meng & Han (1996) explain that the chemistry of ammoniacal leaching for transition metals and their compounds involves not only an oxidation-reduction reaction but also complexation equilibria. The phase relationship between various states of transition metals in aqueous systems can be best identified using stability diagrams, i.e. Pourbaix (Eh-pH) diagrams.

It is now necessary to adjust the electrochemical properties of the solution by applying Eh-pH diagrams in order to determine the most stable regions of the ions present in the reactions. The Eh-pH diagrams show the stability regions for the cupric amine and gold thiosulphate complexes (Aylmore & Muir, 2001).

Figure 2-11 shows that the cupric amine complex is most stable within a pH range of 8.5 to 9.5. Higher pH conditions can cause the formation of sulphide, which, in turn, reduce the gold extraction efficiency (Zipperian et al., 1988).

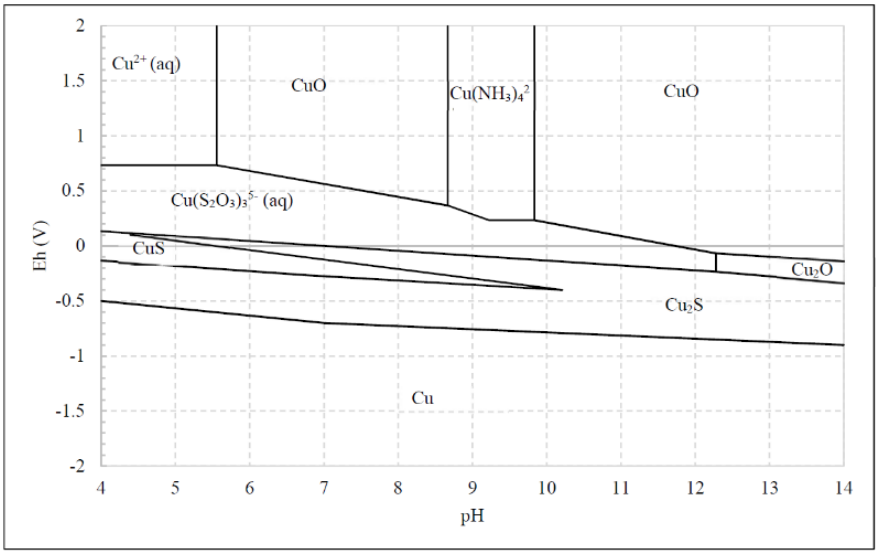

Figure 2-11: Eh-pH diagram at high reagent concentration for Cu-NH_3-$S_2O_3^{2-}$ (Zipperian et al., 1988; Meng & Han, 1996; Aylmore & Muir, 2001; Muir & Aylmore, 2004)

Figure 2-12 shows that the formation of the $Au(S_2O_3)_2^{3-}$ ion is dominant at pH conditions lower than 8.5. According to Hung et al. (2011), due to the activation energy exceeding 25 kJ.mol^{-1}, the reaction is chemically controlled.

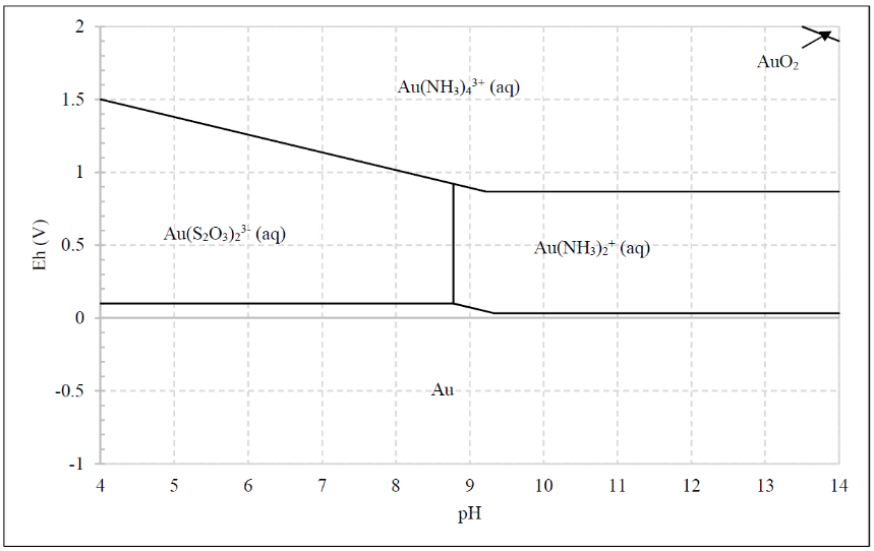

Figure 2-12: Eh-pH diagram at high reagent concentration for Au-NH_3-$S_2O_3^{2-}$ (Zipperian et al., 1988; Meng & Han, 1996; Aylmore & Muir, 2001; Muir & Aylmore, 2004)

Aylmore & Muir (2001) suggested that the increase in gold dissolution in copper thiosulphate solutions containing ammonia is attributed to the stabilisation of the oxidant copper(II) by ammonia forming copper(II) amine. Optimum conditions must be chosen cupric amine stabilisation and sustained gold dissolution can occur.

The Pourbaix diagrams in Figure 2-11 and Figure 2-12 indicate that excessively high pH values favour the precipitation of copper and gold as oxides, which will impede gold extraction. Furthermore, these diagrams show that potential influences equilibria in the leaching system. As an example, the equilibrium between Cu(II) and Cu(I) favours Cu(II) complexes at high potentials and Cu(I) complexes at low potentials. Decreasing the ammonia, thiosulphate and copper(II) concentrations narrows the region of stability of $Cu(NH_3)_4^{2+}$ and $Cu(S_2O_3)_3^{5-}$, and expands the stability region of *CuO*, *Cu_2O* and *Cu_2S* (Aylmore & Muir, 2001).

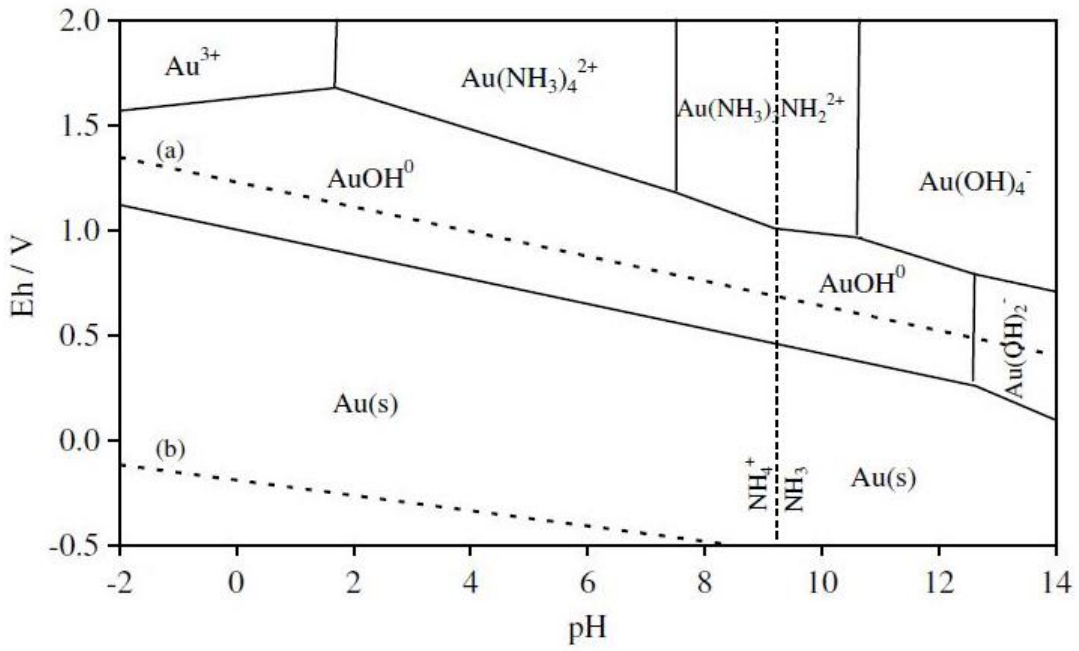

Figure 2-13: Eh-pH diagram at high reagent concentration for Au-NH_3-H_2O (Zipperian et al., 1988; Meng & Han, 1996; Aylmore & Muir, 2001; Muir & Aylmore, 2004)

Figure 2-13 depicts the Pourbaix diagram of the Au-NH_3-H_2O system at 25°C when the total concentration of ammonia is 1.0 M. The aurous ion Au^+ and auric ion Au^{3+} will complex with ammonia to form $Au(NH_3)_2^+$ and $Au(NH_3)_4^{3+}$ complexes. Within the stable region of water, aurous di-amine is the only stable soluble species of gold, while auric tetra-amine is thermodynamically unstable. The ionic gold species are stable over a wide pH range, indicating that gold can be dissolved in ammoniacal solutions even at ambient temperature (Meng & Han, 1996).

2.5.2.2 Temperature

Higher gold dissolution rates have been reported at temperatures ranging between 40-60°C (Aylmore & Muir, 2001; Hung et al., 2011; Ha et al., 2014). In contrast, Abbruzzese et al. (1995) established that increasing the temperature decreased gold recoveries by 20%. They ascribed this result to passivation by cupric sulphide formed by the thermal reaction between Cu(II) ions and thiosulphate. Rath et al. (2003) mentioned that an increase in temperature contributes to a higher extraction rate of gold, but when the temperature exceeds 50°C, the dissolution rate decreases.

Breuer & Jeffrey (2000) and Hung et al. (2011) stated that activation energies lower than 25 $kJ.mol^{-1}$ indicate that the reaction is diffusion-controlled. For temperatures above 40°C, the amount of Cu(II) ions start to decrease. This presents the formation of the cupric amine complex responsible for the oxidation of gold. Ha et al. (2010) reported low gold leaching rates at 20°C but almost complete gold extraction from electronic scrap at 40°C. In their investigation, the corresponding activation energy was found to be 78.6 $kJ.mol^{-1}$, implying a chemically controlled reaction.

2.5.2.3 Thiosulphate Concentration

Thiosulphate is responsible for the dissolution of gold as per reactions (7) and (8). Various studies have reported an increase in leaching efficiency with increasing thiosulphate concentration up to 0.2 M, beyond which the extraction rate decreases (Aylmore & Muir, 2001; Xia & Yen, 2005; Ficeriová et al., 2011).

Ha et al. (2010) stated that at higher thiosulphate concentrations, the thiosulphate consumption increases and degradation occurs, forming products such as sulphate, trithionate and tetrathionate. The variation of thiosulphate concentration changes the gold stability region with a change in pH. If the potential is too low, the formation of a black precipitate of copper sulphide is incurred.

2.5.2.4 Ammonia Concentration

According to Habashi (1993), ammonia can exist in several forms, including free ammonia, ammonium ions and metal amines. For the leaching of base metals, free ammonia can be considered as the active complexing agent and reacts with metal ions. Ammonia increases the rate of gold recovered in the system. An increase in ammonia concentration stabilises copper, and ammonia is involved in the cathodic copper reduction. In the absence of ammonia, the gold dissolution is impeded by sulphur passivation of the gold surface. If ammonia concentration exceeds 0.3 M, the leaching rate decreases, except at copper concentrations less than 0.15 mM. Ammonia prevents gold passivation by being absorbed onto the gold surface, at a higher rate than thiosulphate. At higher pH>9 values, however, the gold dissolution becomes independent of ammonia concentration and is dependent on the thiosulphate concentration, which suggests that the $Au(S_2O_3)_2^{3-}$ complex is more dominant than $Au(NH_3)_2^+$ (Ha et al., 2010).

Aylmore & Muir (2001) suggested that the leaching rate of gold is limited by the diffusion of copper(II) to the surface of gold at low copper concentrations, whereas at higher copper concentrations, the reaction is chemically controlled.
According to Bell et al. (1995), the most significant thiosulphate leaching parameters include temperature, oxygen partial pressure and ammonia concentration.

2.5.2.5 Cupric Ion Concentration

According to Tripathi et al. (2012), the presence of copper ions promotes the dissolution of gold in the thiosulphate solution. The copper present is used as a catalyst agent. Breuer & Jeffrey (2002) state that a typical thiosulphate leaching system will have its potential increased from 65 mV to 238 mV with the addition of copper. This verifies the importance of copper as an oxidative reagent in the solution chemistry and proves that the reaction is electrochemically controlled. The reduction of copper is regarded as a cathodic reaction. Copper reacts with ammonia in an alkaline environment (pH > 9) to form the Cu(II) amine complex which is necessary for the oxidation of gold to gold to the gold thiosulphate complex (Breuer & Jeffrey, 2002).

2.5.2.6 Particle Size

Ficeriová et al. (2011) investigated the effect of particle size on the leaching of gold from PCBs. The experimental leaching conditions were kept constant, and the researchers reported 98% gold extraction with crushed PCBs compared to 16% metal recovery with untreated (uncrushed) PCBs. It can thus be argued that a significant increase in gold dissolution can be obtained by decrease the PCB particle size. The most plausible explanation for this phenomenon is that size reduction increases the particle surface area available for interaction with the lixiviant. Furthermore, Cu layers cover most of the surface of a typical PCB, which means that Au will leach with more strain from full-size PCBs (Li & Miller, 2007; Wei et al., 2010).

Birloaga et al. (2013) investigated the effect of particle size on the acidic thioureation of gold from milled central processing units (CPUs) with particle size smaller than 3 and 0.1 mm. The obtained gold extractions were 18.2 and 82%, respectively, showing significant improvement with smaller particle sizes as a result of the improved contact area between the particles and thiourea solution.

2.5.3 Previous Studies on the Thiosulphate Leaching of Gold from E-waste

Table 2-4: Previous research on the thiosulphate leaching of gold from e-waste

Raw Material			**Leaching Conditions**							**Au Extracted (%)**	**Refs**
type	**Au Content**	**Cu Content**	**$S_2O_3^{2-}$ [M]**	**NH_3 [M]**	**Cu^{2+} [M]**	**Temp [°C]**	**pH**	**Time [hrs]**	**S/L Ratio**		
MP-PCBs	0.12 %	35.1%	0.12	0.2	0.02	25	-	2	6.67%	90	(Ha et al., 2010)
WPCBs	0.014%	47.5%	0.5	1.0	0.2	40	-	48	8.89%	98	(Ficeriová et al., 2011)
MP-PCBs	0.021%	56.48%	0.1 ATS	0.04	-	RT	-	8	10 g/L	56.7 (ground)	(Tripathi et al., 2012)
MP-PCBs	0.021%	56.48%	0.1 ATS	0.04	-	RT	-	8	10 g/L	78.8 (full-size)	(Tripathi et al., 2012)
MP-PCBs	-	-	0.1	0.3	0.01	30	8.5-11.5	4	1/25	50 (full-size)	(Kasper & Veit, 2015)
PC-PCBs	21 g/t	-	0.3	0.38	0.038	23	8.5-11.5	6.75	10.79%	92.2	(Isildar et al., 2017)

MP-PCBs	142-700 g/t	-	0.12	0.2	0.02	30	10	4	1/25	70	(Kasper & Veit, 2018)
MP-PCBs	142-700 g/t	-	0.12 ATS	0.2	0.02	30	10	4	1/25	75	(Kasper & Veit, 2018)
MP-PCBs	-	-	0.5	1.2	0.04	25	10	4	1/4	95.3	(Xiang et al., 2018)
MP-PCBs	453.4 g/t	237 kg/t	0.7	-	-	RT	10.5	6	5%	81	(Gámez et al., 2019)

WPCBs: waste printed circuit boards
MP-PCBs: waste mobile phone printed circuit boards
PC-PCBs: waste computer printed circuit boards
ATS: ammonium thiosulphate
RT: Room temperature
S/L: solid-to-liquid ratio

2.6 Shrinking-Core Model for the Predictive Analysis of Thiosulphate Leaching

According to Levenspiel (1999), modelling has been used in various leaching operations to gain an understanding of the process and assist in decision making. Several models have been applied over the years for leaching of various minerals. The shrinking-core model (SCM) has seen extensive use in the description of liquid-solid reactions, with applications in gold cyanidation, zinc dissolution, manganese, uranium and copper leaching processes (Crundwell & Godorr, 1997; Gbor & Jia, 2004; Othusitse & Muzenda, 2015). Beolchini et al. (2001) incorporated the SCM into the development of a rate expression which describes the leaching of gold ores. Subsequent studies have also included the SCM in the analysis on the effects of particle size distribution in leaching reactors and in predicting the leaching behaviours of high carbonate ores (Crundwell et al., 2013; Kacham & Suri, 2014).

The shrinking-core model assumes that the reaction occurs on the outer layer of the solid particle and proceeds towards the centre of the particle, thereby leaving behind a fully reacted inert solid or ash (Figure 2-14). Thus, the unreacted material is surrounded by the ash layer and is assumed to shrink uniformly throughout the reaction. It is worth noting that the SCM describes two particle behaviours: (i) shrinking particles and (ii) unshrinking particles, which differ based on the formation of the ash layer (Levenspiel, 1999).

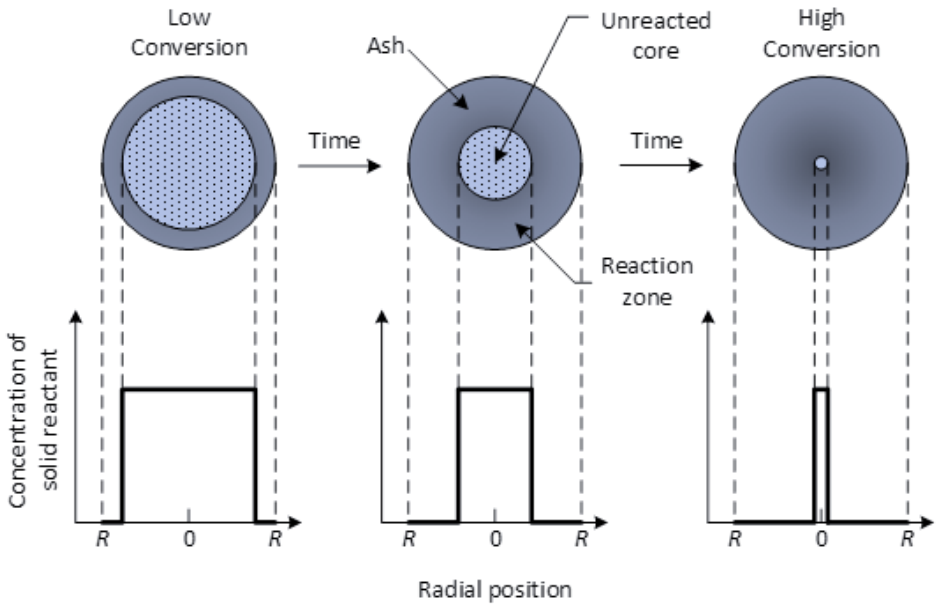

Figure 2-14: Illustration of unreacted core shrinking as the reaction takes place from the outer layer (Levenspiel, 1999)

The shrinking-core model outlined in this section is exclusively applied to constant-size particles. Considering the following reaction between a solid A surrounded by a fluid B:

$$A(f) + bB(s) \longrightarrow products \tag{9}$$

The model is developed by visualising five basic steps occurring during the reaction (Figure 2-15).

Step 1: Diffusion of fluid reactant A through the film layer surrounding the particle to the surface of the solid.

Step 2: Penetration and diffusion of A through the blanket of ash to the surface of the unreacted core.

Step 3: Reaction of fluid A with solid at this reaction surface.

Step 4: Diffusion of fluid products through the ash back to the exterior surface of the solid.

Step 5: Diffusion of fluid products through the film layer back into the main body of the fluid.

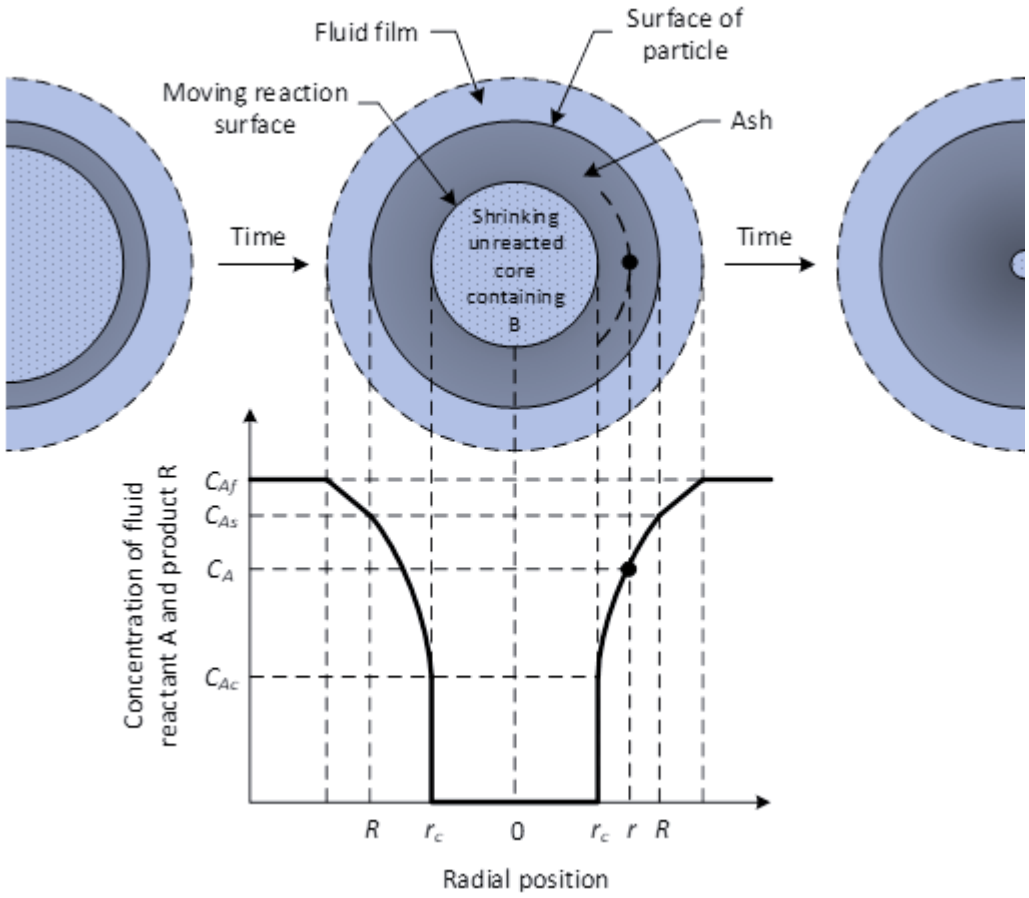

Figure 2-15: Representation of concentration profiles of reactants and products for the reaction of fluid and solid for a particle of unchanging size (Levenspiel, 1999)

In some situations, it can be argued that steps 4 and 5 do not exist because no fluid products are formed. Thus, steps 4 and 5 do not directly contribute to the resistance to the reaction. The resistance is known to change significantly from one step to another, and thus the rate-limiting step in the process will be the one with the highest resistance.

Table 2-5: Shrinking-core model for unshrinking particles (Levenspiel, 1999)

Sphere	**Film Diffusion Control**	**Ash Diffusion Control**	**Reaction Control**
$X_B = 1 - \left(\frac{r_c}{R}\right)^3$	$\frac{t}{\tau} = X_B$ (10) $\tau = \frac{\rho_B R}{3bk_f C_{Af}}$ (11)	$\frac{t}{\tau} = 1 - 3(1 - X_B)^{2/3} + 2(1 - X_B)$ (12) $\tau = \frac{\rho_B R^2}{6b\mathcal{D}_e C_{Af}}$ (13)	$\frac{t}{\tau} = 1 - (1 - X_B)^{1/3}$ (14) $\tau = \frac{\rho_B R}{bk" C_{Af}}$ (15)

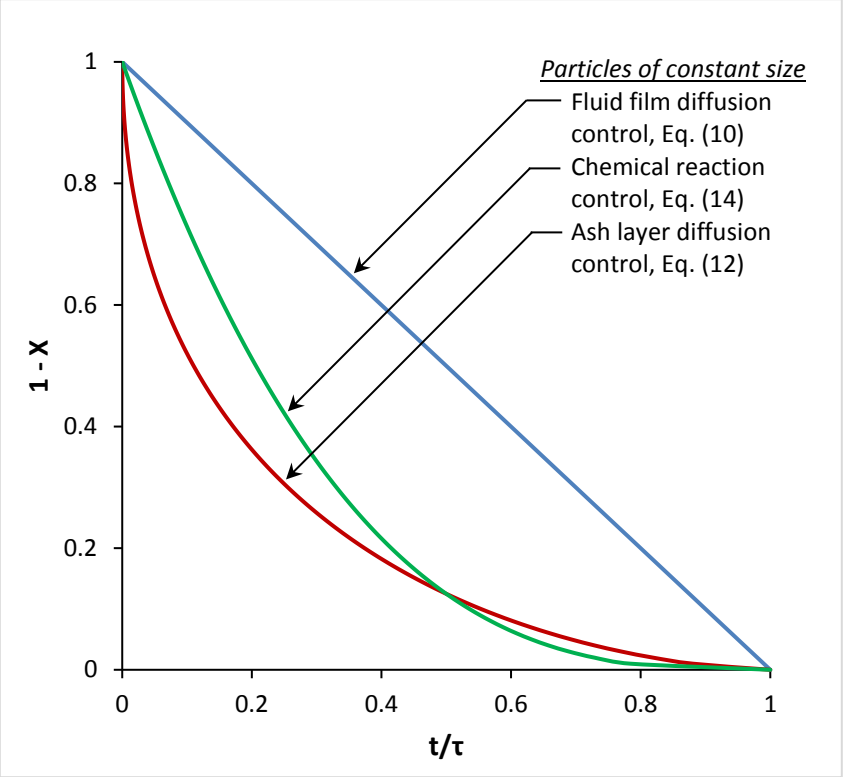

Figure 2-16: Conversion-time profiles of a solid-fluid reaction: SCM for unshrinking spherical particles (Levenspiel, 1999)

The SCM conversion-time expressions for unshrinking particles are provided in Table 2-5 and graphed in Figure 2-16. X and t/τ represent conversion and the fractional time for complete conversion. The variable (1 – X) describes the shrinking of the unreacted core and is directly linked to the conversion. As the reaction progresses, the gradual increase in conversion is accompanied by a reduction of the unreacted core until all the solid reactant is converted and the remaining particles are converted to ash. The SCM is expressed in terms of unreacted core shrinking and fractional time for complete conversion to assist in the determination of the rate-limiting step of the reactive system (Levenspiel, 1999; Othusitse & Muzenda, 2015). Detailed mathematical derivation of the shrinking-core model is provided in Appendix D (section D.3).

2.7 Previous Work on the Shrinking-Core Model in Hydrometallurgy

Several studies have used the shrinking core model directly for the determination of leaching mechanisms. Gbor et al. (2000) used the SCM to describe the behaviour of Co and Ni in the SO_2 leaching of nickel smelter slag. The Co extraction was found to be controlled by ash diffusion and surface chemical reaction, whereas the mechanism of Ni extraction was based on ash diffusion only. These results were confirmed by SEM-EDS analysis. Didyk-Mucha et al. (2016) investigated the application of the SCM to the leaching of serpentinite in sulphuric acid. The process was found to occur in two steps: the surface dissolution of serpentinite particles, followed by surface chemical reaction. The SCM was found to describe only the second stage of the serpentinite leaching process. Khezri et al. (2020) applied the shrinking core and shrinking particle models to assess the reaction mechanism of the leaching of a chalcopyrite concentrate in glycine. The leaching process was found to be controlled by diffusion of the reagents from the product layer in a temperature range of 30 to 60 °C. The rate-limiting step was confirmed by an activation energy of 37.42 kJ/mol, as determined through the Arrhenius plot.

Other studies outlined the modification of the shrinking-core model based on the type of ore and leaching system. Veglio et al. (2001) modified the SCM for the leaching of manganiferous ore with sulphuric acid and lactose (reducing agent) to consider the changing reagent concentrations and reaction rate in relation with the MnO_2 conversion. The modified model accounted for the stoichiometry of the leaching process, and the relationship between reaction rate and conversion was assessed using a variable activation energy approach. The model was found to be a good fit at specific particle sizes but failed to describe the effect of particle size on the dissolution process. Velardo et al. (2002) developed a two-layer shrinking-core (TLSC) model to assess the functional relationship between the leaching rate and reagent concentrations. The modified SCM included adjustable parameters related to the surface diversity of solid particles and was found to provide a satisfactory technique for estimating the order of the leaching reaction. Safari et al. (2009) developed a mathematical model based on the SCM for the leaching of zinc from a zinc ore containing silica. They established that adding the mass transfer resistance due to the thin gelatinous layer covering the reacting core significantly improved the model predictions. It was determined that lower temperatures shifted the control regime to diffusion whereas chemical reaction and diffusion controlled the leaching process at high temperatures.

2.8 Particle Size Distribution and Shrinking-Core Model

The SCM, as discussed in section 2.6, implies that the control regime of a leaching process can be determined without accounting for the effect of particle size distribution because the model assumes mono-sized particles. The process is chemically controlled when there is a linear relationship between the expression $1-(1-X)^{1/3}$ and time (t). The process is controlled by ash diffusion when there is a linear relationship between $1-3(1-X)^{2/3}+2(1-X)$ and t, and when X and t are linearly correlated, the leaching system is controlled by fluid film diffusion (Levenspiel, 1999).

However, an erroneous conclusion as to the control regime of the process can be reached when the PSD is neglected (Gbor & Jia, 2004). This section discusses the incorporation of PSD into the SCM and assesses errors and shifts in the leaching control regime.

For mono-sized particles of diameter D, Table 2-5 indicates that the unreacted fraction is given by:

$$1-X=f(D,t) \tag{16}$$

For a chemically controlled leaching process,

$$f(D,t)=1-X=\left(1-\frac{k_{rn}t}{D}\right)^3 \tag{17}$$

where $k_{rn}=k_rD$ and $k_r=1/\tau$

For ash diffusion control, $f(D,t)$ cannot be expressed algebraically for each D but its value can be obtained from equation (12) written as:

$$1-3(1-X)^{2/3}+2(1-X)=\frac{k_{dn}t}{D^2} \tag{18}$$

where $k_{dn}=k_dD^2$ and $k_d=1/\tau$

For liquid film diffusion control,

$$f(D,t) = 1 - X = \left(1 - \frac{k_{mn}t}{D}\right) \tag{19}$$

where $k_{mn} = k_d D$ and $k_m = 1/\tau$

For a group of particles of various sizes divided into discrete size ranges,

$$Unreacted\ Fraction = \sum_D [f(D,t)]\ x_D \tag{20}$$

where x_D is the mass fraction of size D.

For a continuous distribution of particles,

$$Unreacted\ Fraction = \int_0^\infty [f(D,t)]\ [p(D)]\ dD \tag{21}$$

where

$$f(D,t) = 1 - X, \quad 0 < D < D_t \tag{22}$$

$$f(D,t) = 1 - X = g(D,t), \quad D_t < D < D_{max} \tag{23}$$

$p(D)$ is the particle size density function based on particle mass. D_{max} is the largest particle in the system. $g(D,t)$ represents $f(D,t)$ in equations (17)-(19) for each control scheme. $D_t = k_{rn}t$ for chemical reaction control, $D_t = (k_{dn}t)^{0.5}$ for ash diffusion control, and $D_t = k_{mn}t$ for liquid film diffusion.

Equations (22) and (23) indicate that at any time (t), all particles with sizes less than D_t are converted completely and thus have a conversion X of 1, whereas particles with sizes greater than D_t are partly converted with a conversion expressed by equation (23).

Several models have been used to describe particle size distribution. They are provided in Table 2-6.

Table 2-6: Common particle size distribution functions (Herbst, 1979; Gbor & Jia, 2004; Crundwell et al., 2013)

Name	Gates-Gaudin-Schuhmann	Rosin-Rammler	Log-normal	Gamma
Density function, $p(D)$	$m\frac{D^{m-1}}{D_{max}^{m}}$	$\frac{m}{L^m}D^{m-1}\exp\left[-\left(\frac{D}{L}\right)^m\right]$	$\frac{1}{(2\pi)^{1/2}DZ}\exp\left[-\frac{\log^2(D/L)}{2Z^2}\right]$	$\frac{1}{\beta^\alpha\Gamma(\alpha)}D^{\alpha-1}e^{-D/\beta}$
Distribution function, $P(D)$	$\left(\frac{D}{D_{max}}\right)^m$	$1-\exp\left[-\left(\frac{D}{L}\right)^m\right]$	Numerical integration of density function	
Range, $[D_{min}-D_{max}]$	$[0, D_{max}]$	$[0,\infty]$	$[0,\infty]$	$[0,\infty]$
Mean, μ	$\frac{m}{m+1}d_{max}$	$L\Gamma\left(\frac{m+1}{m}\right)$	$L\exp\left(\frac{Z^2}{2}\right)$	$\alpha\beta$
Variance, σ^2	$\left[\frac{m}{m+2}-\frac{m^2}{(m+1)^2}\right]d_{max}^2$	$L^2\left[\Gamma\left(\frac{m+2}{m}\right)+\Gamma^2\left(\frac{m+1}{m}\right)\right]$	$L^2[\exp(2Z^2)-\exp Z^2]$	$\alpha\beta^2$
Covariance, $CV=\sigma/\mu$	$\frac{\frac{m}{m+2}-\frac{m^2}{(m+1)^2}}{\frac{m}{m+1}}$	$\frac{\left[\Gamma\left(\frac{m+2}{m}\right)+\Gamma^2\left(\frac{m+1}{m}\right)\right]^{0.5}}{\Gamma\left(\frac{m+1}{m}\right)}$	$\frac{[\exp(2Z^2)-\exp Z^2]^{0.5}}{\exp\left(\frac{Z^2}{2}\right)}$	$\frac{1}{\alpha^{0.5}}$

The gamma model is chosen for illustration purposes. Substituting for the gamma function and equations (22)-(23) into equation (21) yields:

$$\begin{aligned} Unreacted\ Fraction &= \int_0^{D_t} 0\frac{1}{\beta^\alpha\Gamma(\alpha)}D^{\alpha-1}e^{-D/\beta}dD \\ &+ \int_{D_t}^{D_{max}} f(D,t)\frac{1}{\beta^\alpha\Gamma(\alpha)}D^{\alpha-1}e^{-D/\beta}dD \end{aligned} \quad (24)$$

The overall conversion can thus be expressed as:

$$X = 1-\int_{D_t}^{D_{max}} f(D,t)\frac{1}{\beta^\alpha\Gamma(\alpha)}D^{\alpha-1}e^{-D/\beta}dD \quad (25)$$

Equation (25) can be used for chemical reaction control and liquid film diffusion control since $f(D,t)$ can be expressed algebraically for these mechanisms. However, for ash diffusion control, the discrete form of equation (25) (i.e., equation (20)) should be used. Equation (25) can be solved numerically using the available third-party computer software packages and libraries.

Gbor & Jia (2004) showed that when the covariance or coefficient of variation CV of particle size distribution can be used to assess whether the PSD can be included in and excluded from the shrinking core model when determining the rate-limiting step or control regime of a leaching process. The authors indicated that for CV values less than 0.3, the linear relationship between $1-(1-X)^{1/3}$ and t for chemical reaction control is upheld, and the PSD can be excluded from the SCM. For systems with higher CV values (>0.7), ignoring the PSD erroneously shifts the leaching mechanism from liquid film diffusion to ash diffusion. These results were obtained irrespective of the PSD model used.

CHAPTER 3

RESEARCH METHODOLOGY

CHAPTER 3 : RESEARCH METHODOLOGY

In this chapter, the details are given regarding the use of equipment and materials, as well as experimental procedures followed during all experimental runs conducted. Descriptions of the instruments used are also included.

3.1 Research Design

A quantitative experimental approach was used in this research. The experiments were grouped into three parts (Figure 3-1): the size reduction of PCBs by grinding, aqua regia leaching and the ammonium thiosulphate leaching experiments.

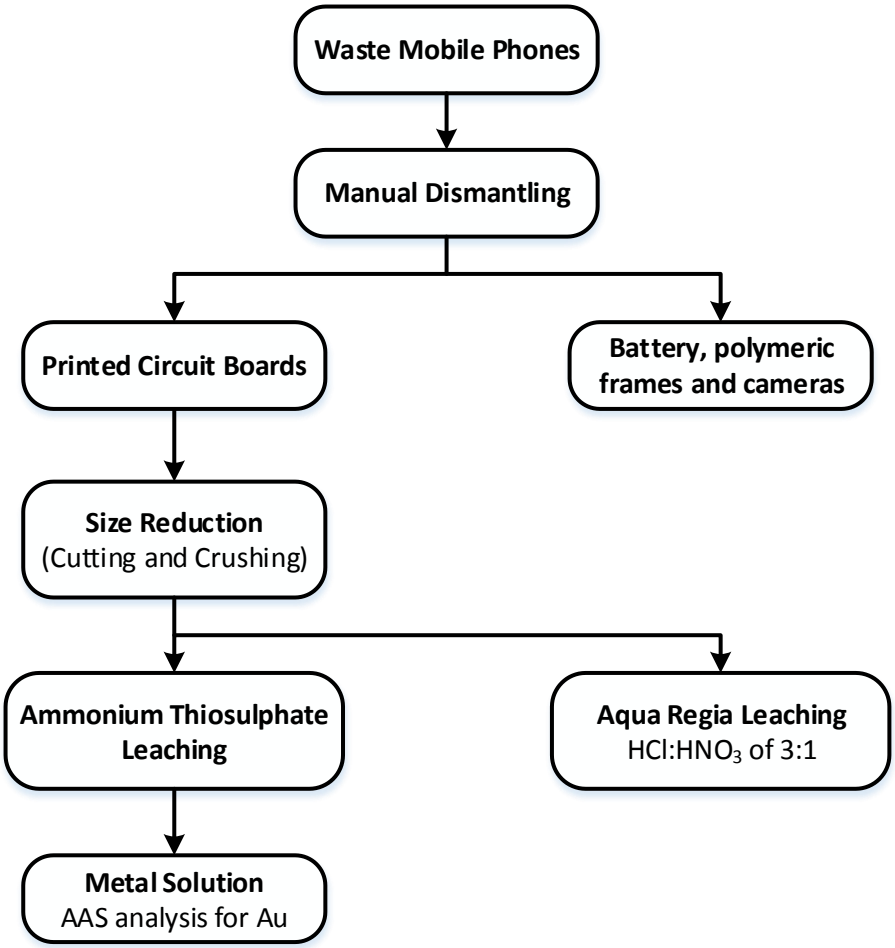

Figure 3-1: Flowchart of the research methodology

3.1.1 PCB Size Reduction

Unused mobile phones of different makes and models were collected from various local mobile phone outlets. The mobile phones were dismantled manually using a screwdriver. The PCBs were separated from the battery, polymeric frames and cameras. The physical pre-treatment involved the size reduction of all mobile phone PCB scrap. The scrap was not separated in terms of metals and non-metals, but it was directly shredded to four different PSD samples.

3.1.2 Aqua Regia Leaching

The gold content of PCBs was determined by aqua regia leaching. A 32 wt% stock HCl solution was added to an empty beaker, followed by the slow addition of a 55 wt% HNO_3 stock solution. The volumes of these acid solutions were added to make up a 40-mL lixiviant solution to obtain a mixture molar ratio of 1:3. The leaching solution was heated to 60°C before slowly adding a 5-g PCB sample. The leaching process was carried out for 24h under a fume cupboard. The procedure was replicated three times, and leachate samples were collected at the end of the process for gold analysis by atomic absorption spectroscopy (AAS).

3.1.3 Ammonium Thiosulphate Leaching

Experimental Conditions

The thiosulphate leaching experiments according to a one-factor-at-a-time design approach (Table 3-1) consisting of two numeric factors: particle size distribution (PSD) and pulp density (PD). The PSD had four levels that mirrored the conditions for coarse and fine particles. The pulp density had three levels: 40, 80 and 120 g/L. The reagent concentrations, pH, temperature and mixing rate were fixed, as shown in (Table 3-2). The gold conversion (extraction) was the response investigated in the thiosulphate leaching studies.

Table 3-1: Experimental design of thiosulphate leaching

	Factor 1	Factor 2	Response
Run	Pulp Density (g/L)	PSD	Gold Conversion
1	80	2	
2	80	4	
3	40	3	
4	120	1	
5	120	4	
6	120	3	
7	40	4	
8	120	2	
9	80	3	
10	40	1	
11	80	1	
12	40	2	

PSD: Particle size distribution

Table 3-2: Fixed experimental parameters (Tripathi et al., 2012)

Parameters	Units	Values
Temperature	°C	30
pH	-	9.5
Redox	mV	200 - 250
Stirring speed	rpm	350
Ammonium thiosulphate	M	0.1
Copper sulphate	M	0.04
Reaction time	hours	3

Experimental Procedure

The thiosulphate leaching experiments were conducted in the batch reactor shown in Figure 3-2. Pre-treated PCB samples were weighed according to the prescribed PSD and pulp density. 14.8 g/L (0.1 M) ammonium thiosulphate and 6.4 g/L (0.04 M) copper (II) sulphate weighted and prepared in the reactor unit. The PCBs were added, and the reaction mixture was adjusted to 500 mL with deionised water. The mixture temperature was adjusted to 30°C, and the solution pH was set and maintained at 9.5 with the aid of ammonia solution. The leaching process was then allowed to proceed for 3 hours, and leachate samples were collected every 30 minutes for metal analysis by AAS.

3.2 Description of Experimental Apparatus

The apparatus and equipment were used during the experimental trials are listed below. The thiosulphate leaching studies were carried out in a 1-Litre reactor unit (Figure 3-2). Leachate samples were collected from the reaction mixture at various experimental conditions (Table 3-1) and subjected to gold analysis by AAS.

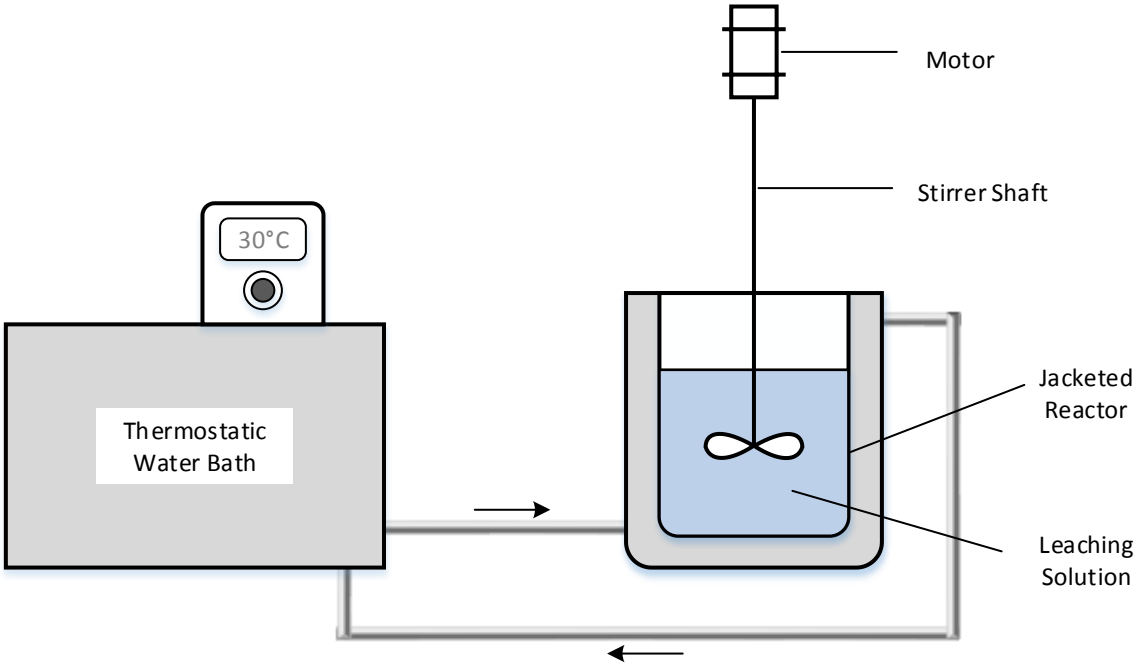

Figure 3-2: Schematic diagram of the leaching experimental setup

- pH probe
- Redox probe
- Batch reactor tank with baffles
- Water bath
- Electronic overhead stirrer
- Pipette
- 10 ml volumetric flask
- 45-micron syringe filters
- Syringe filter
- Atomic Absorption Spectrometer
- Buchner funnel
- Vacuum pump

- Shredding unit
- Metal cutter
- Analytical balance scale
- Heater
- Thermocouple

3.3 Description of Materials

The chemicals (analytical grade) used in this research were supplied by Sigma-Aldrich (Merck) and B & M Scientific.

- Nitric acid (55%)
- Hydrochloric acid (32%)
- Ammonia solution (35%)
- Ammonium thiosulphate
- Copper (II) sulphate
- Gold standard solution
- pH calibration standards (pH 4, 7 and 10)
- Deionised water (DI).

3.3.1 Ammonium Thiosulphate

98% purity ammonium thiosulphate was used as the leaching agent. It is a white crystalline water-soluble solid. Table 3-3 gives detailed specifications of the lixiviant.

Table 3-3: Ammonium thiosulphate specifications

Specification	Percentage Composition
Ammonium Thiosulphate	>98
pH-value (5%, water)	5.0-7.0
Chloride	<0.05
Sulfate and sulphide (as SO_4)	<0.001
Heavy Metals (as Pb)	<0.002
Calcium (Ca)	<0.005
Iron (Fe)	<0.002
Sodium (Na)	<2

3.3.2 Copper Sulphate

Copper sulphate powder was used in the leaching experiments as a metal oxidant. It is a blue crystalline salt and regulates the redox potential of the thiosulphate leaching system. A detailed description of this reagent is provided in Table 3-4.

Table 3-4: Copper sulphate specifications

Specification	Mass Percentage
Copper Sulphate	>99
Insoluble Matter	<0.005
Chloride	<0.001
Total Nitrogen	<0.001
Lead	<0.005

3.3.3 Ammonia Solution

Ammonia solution was used to regulate the pH of the solution. Ammonia is a toxic, reactive, colourless and corrosive compound with a very sharp odour. It deprives the lungs of oxygen and causes suffocation if its vapours are inhaled. It was thus used in a fume cupboard with the appropriate protection equipment (respiratory mask, laboratory gloves, safety goggles and shoes). Only the required amount for adjusting the pH was used at any time instance. A 35% ammonia stock solution was used.

3.3.4 Nitric Acid

Nitric acid is a strong acid which was used in combination with hydrochloric acid to form aqua regia. The concentration of the nitric acid stock solution used was 55%.

3.3.5 Hydrochloric Acid

Hydrochloric acid was used in combination with nitric acid to produce aqua regia. The concentration of the stock solution used was 32%. These acids are extremely corrosive, and thus appropriate health and safety measures were followed when handling these reagents.

3.4 Personal Protection Equipment

All experimental runs were conducted in a fume cupboard, and strict health and safety protocols were always implemented. The following personal protective equipment was used:

- Chemical grade respiratory mask
- Safety goggles
- PVC and standard disposable nitrile examination gloves
- Lab coats
- Safety shoes.

CHAPTER 4

RESULTS AND DISCUSSION

CHAPTER 4 : RESULTS AND DISCUSSION

4.1 Particle Size Distributions

The PCB preconditioning stage was concerned with the solid size reduction to less than 2 mm, as prescribed by the existing literature (Ficeriová et al., 2011; Tripathi et al., 2012; Behnamfard et al., 2013; Birloaga et al., 2013; Isildar et al., 2017). The solid waste was subjected to crushing, milling and sieving to obtain four particle size distributions (PSDs) that reflected the conditions of coarse and fine particles. The four PSD and corresponding median (D_{50}) and mean sizes are shown in Figure 4-1. The particle size is decreased from median and mean sizes of 592 and 658 µm to 354 and 433 µm. The median size was determined graphically from the cumulative undersize distributions while the mean size was obtained by fitting the *Gates-Gaudin-Schuhmann (GGS)* and *Rosin-Rammler (RR)* models to the PSD data. Numerous studies have employed these models to describe the size distribution of solid particles (Herbst, 1979; Gbor & Jia, 2004; Crundwell et al., 2013).

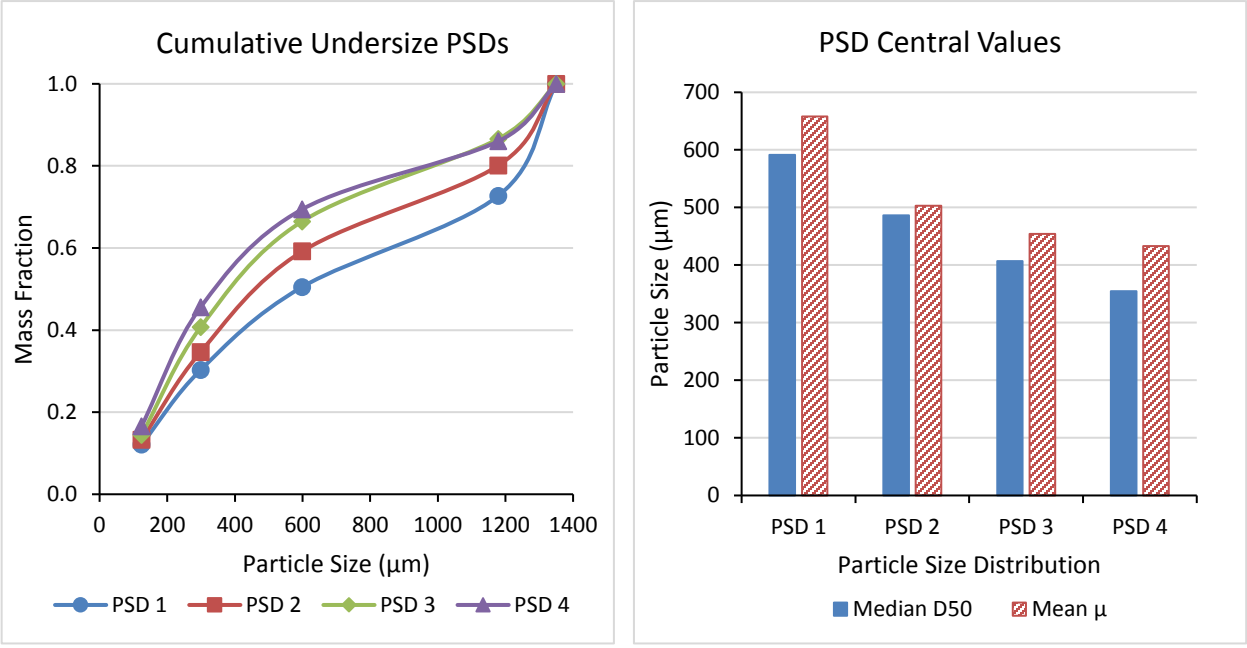

(a) (b)

Figure 4-1: (a) Cumulative particle size distributions, (b) PSD median D_{50} and mean levels

Not only were the GGS and RR models used to estimate the mean size of the PSDs, but they were also used to determine covariances based on the best model fit to the data. It is noteworthy that the covariance were used to assess the requirement of incorporating the PSD into the SCM characterisation of the leaching process which is further discussed in section 4.4.

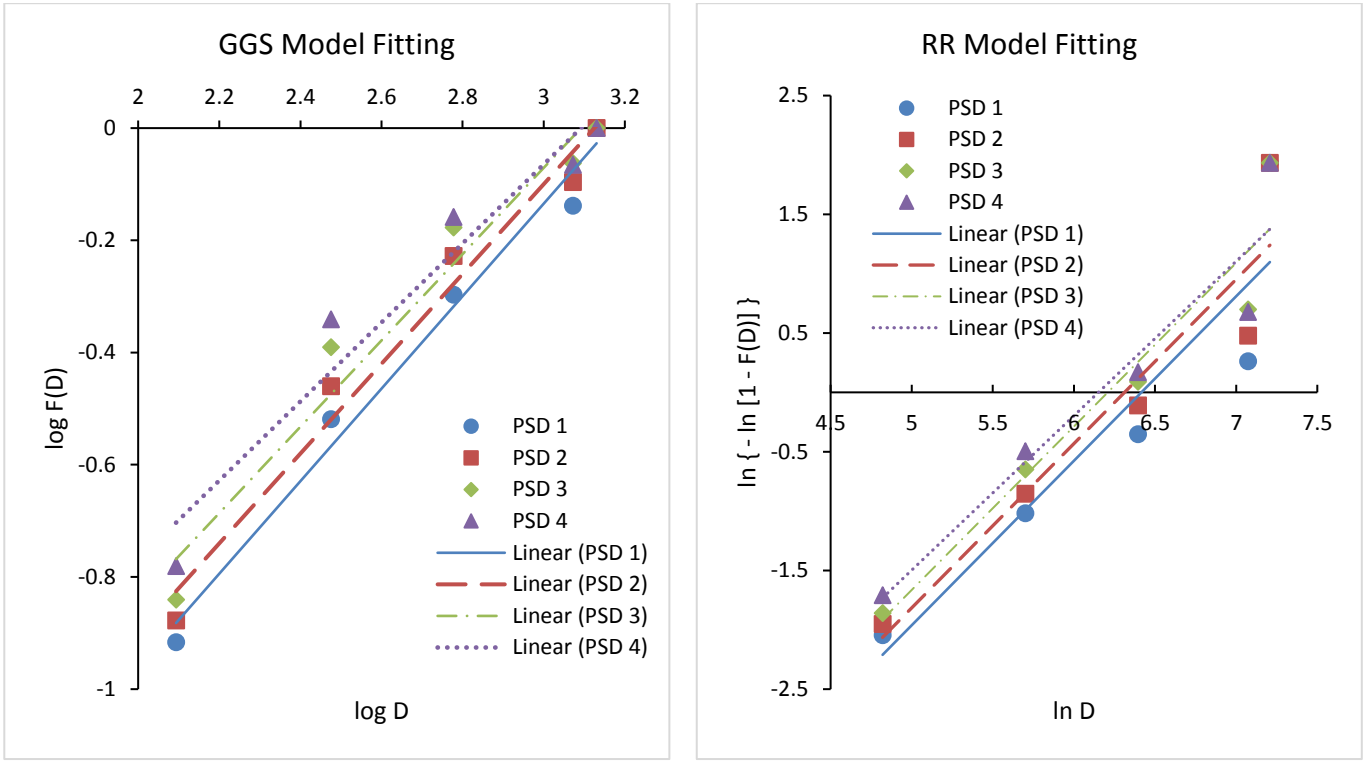

(a) (b)

Figure 4-2: Fitting of PSD data to (a) Gates-Gaudin-Schuhmann (GGS) model and (b) Rosin-Rammler (RR) model

Figure 4-2 shows the fitting of the PSD data to the GGS and RR models. In addition, the PSD parameters for GGS and RR models, as well as their corresponding coefficients of determination R^2 and covariances CV are provided in Table 4-1. From the observations in Figure 4-2 and the R^2 values obtained, it can be inferred that the GGS model closely describes the largest particles at PSD 1. The other PSDs can be represented by the two models based the R^2 values alone. However, an examination of Figure 4-3 suggests that RR model is a better fit for PSD 2 to 4 by virtue of the closeness of predicted and actual median (D_{50}) sizes compared to the GGS model. Figure 4-3 also confirmed the better fit of the GGS model to PSD 1 based on the closeness of the predicted to the actual D_{50} values compared to the RR model. These results are in accordance with the literature in that the GGS and RR models have been reported to characterise the size distribution of large and small particles, respectively (Gbor & Jia, 2004; Ahmed & Ahmed, 2008).

The covariance of each PSD was determined from the model that was best fit to the data. It was found to be ~0.2 for PSD 1 based on the GGS model, and ~0.3 for the other PSDs based on the RR model.

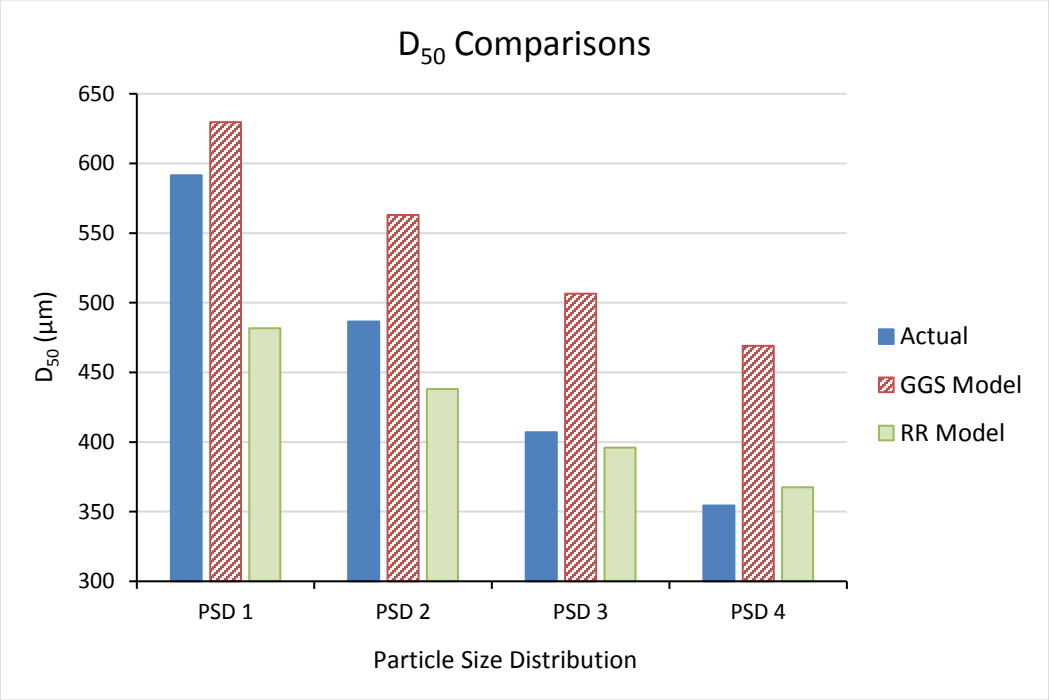

Figure 4-3: Comparison of D_{50} values obtained from actual PSDs, Gates-Gaudin-Schuhmann and Rosin-Rammler models

Table 4-1: Summary of PSD parameters obtained from GGS and RR models, and corresponding correlation coefficients and covariances

	Gates-Gaudin-Schuhmann (GGS) Model				**Rosin-Rammler (RR) Model**			
PSD	m	$D_{max}\ (\mu m)$	R^2	**Covariance *CV***	m	$L\ (\mu m)$	R^2	**Covariance *CV***
PSD 1	0.8246	1456	0.9833	**0.1940**	1.3856	611	0.8588	0.3088
PSD 2	0.8004	1333	0.9762	0.1983	1.3837	551	0.8968	**0.3084**
PSD 3	0.7694	1236	0.9577	0.2041	1.3772	497	0.9277	**0.3070**
PSD 4	0.7046	1235	0.9442	0.2169	1.3010	469	0.9161	**0.2879**

These results are discussed in connection with the gold extraction and the shrinking core model in the remainder of the chapter.

4.2 Gold Extraction

The thiosulphate leaching experiments followed a one-factor-at-a-time design approach consisting of two numeric factors or independent variables. The first factor was particle size distribution with four levels that mirrored the conditions of coarse and fine particles. The second factor was pulp density with three levels: 40, 80 and 120 g/L. The lixiviant concentration and other leaching parameters were fixed, as established in chapter three (Table 3-2). The gold extraction (conversion) was the investigated response or dependent variable. The PCBs contained 172 g Au/ton-PCB based on the aqua regia characterisation.

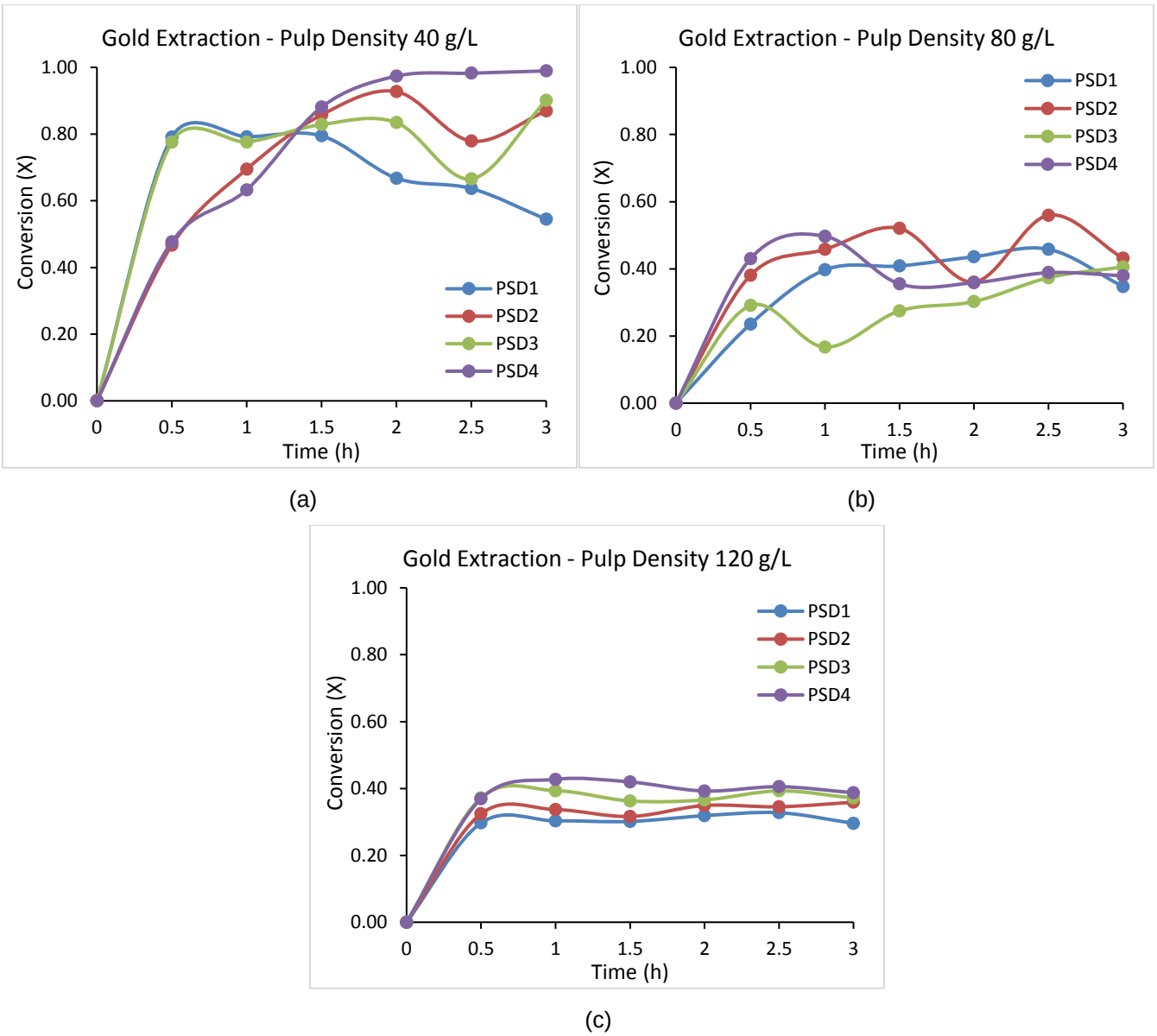

Figure 4-4: Gold conversion in ammonium thiosulphate leaching [0.1 M $S_2O_3^{2-}$, 0.04 M Cu^{2+}, pH 9.5, 30°C, 350 rpm stirring, 3 hours]: (a) 40 g/L PD, (b) 80 g/L PD and (c) 120 g/L PD

Figure 4-4 shows the gold conversion profiles at the investigated conditions. The effects of varying the pulp density were substantial in terms of gold extraction. The pulp density increased the gold extraction, irrespective of the PSD used. Reducing the pulp density from 120 to 40 g/L improved the gold dissolution from average values of 35 to 80 %. The highest metal conversion of 97% was obtained in 2 hours of leaching time at 40 g/L pulp density and PSD 4 (D_{50} 354 µm and mean 433 µm). Classic leach kinetics theory explains that finer particles yield higher overall recovery of the valuable metal by virtue of the increased specific surface area of contact between the PCB and leaching solution. Increasing the pulp density resulted in an excess of PCB solids, and thus rendering thiosulphate the limiting reagent. Furthermore, low pulp densities would further increase the leaching efficiency by improving the contact between the solid and liquid phases and increasing the availability of the lixiviant for the leaching reaction to proceed with no impediment. These results are on par with previous studies as outlined in Table 2-4 where lower gold conversion were obtained at higher pulp densities when reagent concentrations were similar to those used in the current research project.

The particle size distribution had a significant impact on the gold extraction at the lowest pulp density of 40 g/L. The gold conversion was found to increase with a decrease in particle size, with the highest extraction of 97% achieved at median and mean sizes of 354 and 433 µm, respectively. Higher pulp densities, on the other hand, were less sensitive to changes in PSD. The gold extraction was found to oscillate between 40 to 50% at 80 g/L pulp density and from 35 to 40% at 120 g/L pulp density, with no distinct behavioural pattern of gold extraction with PSD variation. At higher pulp densities, the thiosulphate leaching process is impeded as results of the excess solids, thus making the dissolution process inefficient. In addition, high pulp densities can favour the co-dissolution of neighbouring metals such as Ag, Cu and Pb present in the PCBs.

Therefore, based on the experimental results presented in Figure 4-4, it can be inferred that the effect of the pulp density variation was more pronounced than particle size distribution variation in terms of gold extraction. More insights into the factor effects on gold extraction were obtained through statistical analysis and outlined in section 4.3.

4.3 Statistical Analysis of Leaching Results

A *two-factor Anova (analysis of variance) without replication* was conducted to establish the main factor effects. The estimated marginal means of gold extraction were used to assess and compare the effect size of each factor investigated. The null hypothesis H_0 of the Anova was that the factor variations were not statistically significant with respect to the response variable. The alternative or research hypothesis H_a was that the factor variations had a statistically pronounced impact on the response variable (DeCoursey, 2003; Montgomery, 2017).

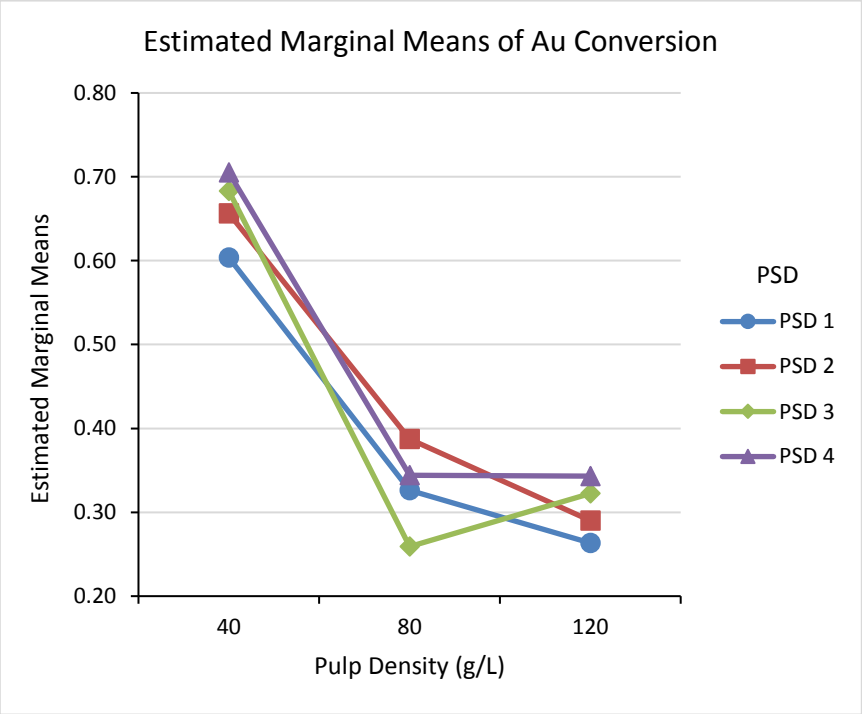

Figure 4-5: Factor effect size comparison - estimated marginal means of gold extraction

The Anova results of the thiosulphate leaching experiments are tabulated in Appendix B (Table B-5). The pulp density variation was found to be statistically significant (p-value 0.00003 << alpha 0.05 and F-statistic 90.64 > F-critical 5.14) whereas the variation of particle size distribution had no statistically significant impact on gold extraction (p-value 0.33 > 0.05 and F-statistic 1.41 < F-critical 4.76). This observation was in agreement with the previous discussion in section 4.2 which indicated that varying the pulp density saw a significant improvement in gold extraction while the effect of PSD variation was not evident, specifically at high pulp densities. For the lowest pulp density (40 g/L), however, the effect of varying the particle size distribution from PSD 1 to 4 (larger to finer particles) had a significant impact on improving the gold extraction.

Overall, the estimated marginal means of gold extraction (Figure 4-5) also supported the higher significance of the pulp density variation compared to PSD by virtue the higher variability in gold extraction obtained at different pulp densities compared to different PSDs.

4.4 Particle Size Distribution, Shrinking-Core Model and Rate-limiting Mechanism

The remainder of this Chapter discusses the implications of particle size distribution on the shrinking core model for the determination of the leaching mechanism or control regime.

4.4.1 Assumptions and Considerations of Goodness of Fit Analysis

The following simplifying assumptions and considerations were adopted in the goodness of fit analysis.

- The PCBs were spherical and conserved their sphericity during the leaching experiments.
- The particles retained that sizes during the leaching process. This assumption is supported by the low gold content in PCBs, which would not affect the total PCB mass even if complete conversion were achieved.

4.4.2 Particle Size Distribution in SCM Characterisation

The aim of this research was to assess the effect of incorporating the PSD into the shrinking core model with regards to the determination of the control regime of the leaching process. Gbor & Jia (2004) suggested that the decision to include the PSD into the SCM should be based on the covariance of the PSD data. The PSD should be neglected for CV values less than 0.3, but for CV values greater than 0.3 the PSD should be included in the SCM to avoid mistakenly identifying the rate-limiting step of leaching. This criterion should be applied irrespective of the mathematical model used to describe the PSD. The CV values of the particle size distribution used in this research were found to be less than 0.3, as outlined in section 4.1 (Table 4-1). Therefore, the shrinking core model was safely fitted to conversion data without accounting for particle size distribution.

4.4.3 SCM fitting to Thiosulphate Leaching Data

Figure 4-6 shows that at the lowest pulp density (40 g/L), the shrinking core model was found to fit the leaching data only for the smallest particles at PSD 4 (D_{50} 354 µm and mean 433 µm) based on the coefficients of determination obtained. Under these conditions, the process was found to be controlled by chemical reaction (R^2 0.9535) and ash/inert layer diffusion (R^2 0.9422). The liquid film diffusion model exhibited the lowest correlation (R^2 0.8177), and thus was not a good fit for the leaching data. The existing body of literature concurs that in a typical leaching system with unshrinking particle and shrinking unreacted core, the film diffusion control has the lowest impact on the extraction process, while the reaction control and ash diffusion control have a higher influence on the description of the process (Levenspiel, 1999; Liddell, 2005). This stems from the fact that, as the reaction progresses, the reacted ash gradually increases in size and thus increasingly opposes the diffusion of the lixiviant from the liquid-phase to the unreacted core surrounded by this inert ash (ash diffusion control). In chemical reaction control, the leaching process progresses according to the fundamental electrochemical and thermodynamic aspects of the process, as discussed in chapter two (section 2.5.2.1). On the other hand, the dissolution process of larger particles at PSD 1 to 3 (median sizes of 592 to 407 µm and mean sizes of 658 to 454 µm) could not be described by any of the control regimes prescribed by the shrinking core model.

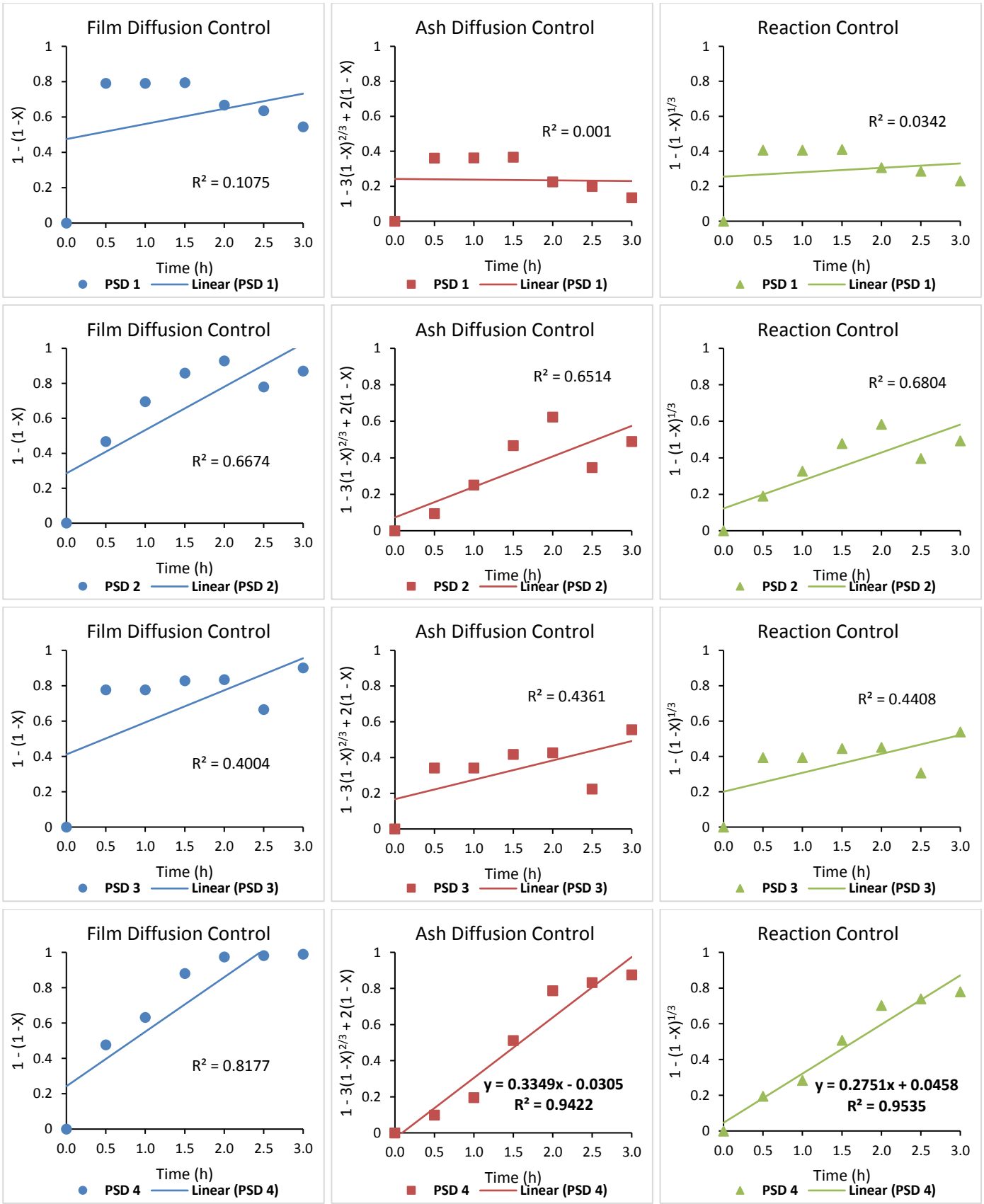

Figure 4-6: Fitting of SCM to leaching experimental data for 40 g/L pulp density

At higher pulp densities (80 and 120 g/L), the unreacted core size reductions did not reach satisfactory levels, irrespective of the PSD level. None of the predictive mechanisms of the SCM fitted the kinetic data (see model fitting plots in Figure C-1 and Figure C-2 of Appendix C). The observation was confirmed statistically based on the lack of correlation (low R^2 values) obtained at 80 and 120 g/L pulp densities. High pulp densities hindered the shrinking of the unreacted core and corresponding gold conversion. Furthermore, they impeded the application of the shrinking-core model to describe, predict and provide insight into the rate-limiting mechanism of the leaching process. On the other hand, The PSD variation did nothing to alleviate or counteract the impending character of high pulp densities.

Possible explanation for the SCM not fitting the leaching data, for larger particles at low pulp density and all particle sizes at higher pulp densities, is that the leaching kinetics under these conditions could have been impacted by any of the following factors (which were not accounted for in this research): (i) the SCM assumes that a single overall parameter, the effective diffusivity (including all mechanistic resistances to leaching) can sufficiently describe the mass transfer within a reacting solid particle, which can lead to difficulties in applying the SCM to leaching data (Liddell, 2005); (ii) the pseudo-steady state assumption (PSSA) of the SCM as presented by Levenspiel (1999) suggests that there is a discrete interface between the reacted and unreacted sections in the solid, but this assumption does not apply to all leaching systems (Liddell, 2005); (iii) the effects of particle disruption and partitioning triggered by the mechanical stirring on the leaching kinetics (Velardo et al., 2002).

In conclusion, the thiosulphate leaching of gold from waste mobile phone PCBs was found to be controlled by ADC and RC at the 40 g/L pulp density. The control regime can be further isolated by determining the activation energy of the leaching process (Gbor & Jia, 2004; Crundwell et al., 2013; Khezri et al., 2020).

CHAPTER 5

CONCLUSION AND RECOMMENDATION

CHAPTER 5 : CONCLUSION AND RECOMMENDATION

5.1 Conclusion

This study successfully evaluated the effect of PSD incorporation on the application of shrinking core model to characterise the rate-limiting step of the thiosulphate leaching of gold from waste mobile phone PCBs. It was determined that the PSD could be excluded from the shrinking core modelling based on the PSD covariances obtained (CV < 0.3). This means that the SCM was applied directly to the leaching data, assuming mono-sized particles. The GGS and RR models were used to describe the PSDs used and determine the central values (median and mean sizes) and covariances of the PSDs. The gold extraction was found to reach 97% in 2 hours at 40 g/L pulp density, 0.1 M thiosulphate, 0.04 M copper sulphate, pH 9.5, 30°C and 350 rpm mixing rate. These results were obtained with PCB particles with median and mean sizes of 354 and 433 µm, respectively. The variation of particle size distribution had little to no significant impact on gold extraction at higher pulp densities but did influence gold extraction at low pulp density. Reducing the pulp density resulted in a signification improvement in gold extraction. Based on the shrinking-core model, the thiosulphate leaching of gold from waste mobile phone PCBs was found to be controlled by chemical reaction and ash layer diffusion at 40 g/L pulp density. SCM characterisation could be achieved only at lower pulp density with finer particles.

5.2 Recommendation for Future Research

Based on more recent studies, there has been some contention about the effect of size reduction on the efficiency of the leaching of gold from waste printed circuit boards. Therefore, subsequent research should study the effect of particle size and particle size distribution in a wider size spectrum (from full-size PCBs to micron-scale PCBs) to establish an in-depth understanding of their effects and possibly envisage any interaction between particle size distribution and pulp density. Size analysis should be carried out during the leaching experiments to track changes in PSD for a detailed assessment of the effect of PSD on the leaching process.

More kinetic data points should be collected during leaching experiments for a more comprehensive model fitting. A full factorial design of experiments should be carried out to get more insights into the interactions between particle size distribution, pulp density and other

leaching parameters such as reagent concentrations, pH and temperature. An in-depth metal analysis should be conducted during the leaching experiments to examine properly the behaviour of neighbouring metals in the leaching system.

The covariance of particle size distribution is the reflection of the efficiency and diversity of the size reduction and sieving processes. As such, the PSD range should be widened to improve the assessment of the effect of PSD on the leaching kinetics and the SCM characterisation of the dissolution process.

The leaching mechanism, identified through SCM characterisation, should be confirmed by the determination of the activation energy. Hence the need to vary the temperature during leaching experiments.

BIBLIOGRAPHY

Abbruzzese, C., Fornari, P., Massidda, R., Vegliò, F. & Ubaldini, S. 1995. Thiosulphate leaching for gold hydrometallurgy. *Hydrometallurgy*, 39(1–3): 265–276.

Ahmed, M.M. & Ahmed, S.S. 2008. A comparison study to determine the mean of particle size distribution for truthful characterization of environmental data (part 1). *J. Eng. Sci., Assiut University*, 36(1): 147–166.

Akcil, A., Erust, C., Gahan, C.S., Ozgun, M., Sahin, M. & Tuncuk, A. 2015. Precious metal recovery from waste printed circuit boards using cyanide and non-cyanide lixiviants--a review. *Waste Management*, 45: 258–271.

Anahide, B. 2007. *The Green e-Waste Channel : model for a reuse and recycling system of electronic waste in South Africa*. University of Lausanne.

Antrekowitsch, H., Potesser, M., Spruzina, W. & Prior, F. 2006. Metallurgical recycling of electronic scrap. In *Procedings of the EPD Congress*. San Antonio: 899–908.

Arshadi, M. & Mousavi, S.M. 2015. Enhancement of simultaneous gold and copper extraction from computer printed circuit boards using Bacillus megaterium. *Bioresource Technology*, 175: 315–324.

ATE. 2012. Identification of the Magnitude of Electrical and Electronic (E-Waste) Situation in South Africa: A Strategic approach to international chemicals Management (SAICM) E-Waste as an emerging Policy Issue. http://africainstitute.info/wp-content/uploads/2013/02/E-WASTE-South-Africa-2012.pdf 10 August 2016.

Aylmore, M.G. 2016. Alternative lixiviants to cyanide for leaching gold ores. In *Gold Ore Processing*. Elsevier: 447–484.

Aylmore, M.G. & Muir, D.M. 2001. Thiosulfate Leaching of Gold--a Review. *Minerals Engineering*, 14(2): 135–174.

Babu, B.R., Parande, A.K. & Basha, C.A. 2007. Electrical and electronic waste: a global environmental problem. *Waste Management & Research*, 25(4): 307–318.

Baldé, C.P., Wang, F., Kuehr, R. & Huisman, J. 2015. The global e-waste monitor-2014. *UNU-IAS: Bonn, Germany*.

Baniasadi, M., Vakilchap, F., Bahaloo-Horeh, N., Mousavi, S.M. & Farnaud, S. 2019. Advances in bioleaching as a sustainable method for metal recovery from e-waste: A review. *Journal of Industrial and Engineering Chemistry*.

Behnamfard, A., Salarirad, M.M. & Veglio, F. 2013. Process development for recovery of copper

and precious metals from waste printed circuit boards with emphasize on palladium and gold leaching and precipitation. *Waste Management*, 33(11): 2354–2363.

Bell, S.L., Welch, G.D. & Bennett, P.G. 1995. Development of ammoniacal lixiviants for the in-situ leaching of chalcopyrite. *Hydrometallurgy*, 39(1–3): 11–23.

Beolchini, F., Papini, M.P., Toro, L., Trifoni, M. & Veglio, F. 2001. Acid leaching of manganiferous ores by sucrose: kinetic modelling and related statistical analysis. *Minerals Engineering*, 2(14): 175–184.

Birloaga, I., De Michelis, I., Ferella, F., Buzatu, M. & Veglio, F. 2013. Study on the influence of various factors in the hydrometallurgical processing of waste printed circuit boards for copper and gold recovery. *Waste Management*, 33(4): 935–941.

Biswas, A.K. & Davenport, W.G. 1994. Noranda and Teniente processes. In A. K. Biswas & W. G. Davenport, eds. *Extractive metallurgy of copper*. Amsterdam: Pergamon: 160–178.

Brandl, H., Bosshard, R. & Wegmann, M. 2001. Computer-munching microbes: metal leaching from electronic scrap by bacteria and fungi. *Hydrometallurgy*, 59(2–3): 319–326.

Breuer, P.L. & Jeffrey, M.I. 2002. An electrochemical study of gold leaching in thiosulfate solutions containing copper and ammonia. *Hydrometallurgy*, 65(2–3): 145–157.

Breuer, P.L. & Jeffrey, M.I. 2000. Thiosulfate leaching kinetics of gold in the presence of copper and ammonia. *Minerals Engineering*, 13(10–11): 1071–1081.

La Brooy, S.R., Linge, H.G. & Walker, G.S. 1994. Review of gold extraction from ores. *Minerals Engineering*, 7(10): 1213–1241.

Burns, D.T., Townshend, A. & Carter, A.H. 1981. *Inorganic reaction chemistry: Reactions of the elements and their compounds. Part B: Osmium to Zirconium*. Ellis Horwood.

Camelino, S., Rao, J., Padilla, R.L. & Lucci, R. 2015. Initial studies about gold leaching from printed circuit boards (PCB's) of waste cell phones. *Procedia Materials Science*, 9: 105–112.

Chehade, Y., Siddique, A., Alayan, H., Sadasivam, N., Nusri, S. & Ibrahim, T. 2012. Recovery of gold, silver, palladium, and copper from waste printed circuit boards. In *International Conference on Chemical, Civil and Environment engineering (ICCEE'2012)*. 226–234.

Chi, T.D., Lee, J., Pandey, B.D., Yoo, K. & Jeong, J. 2011. Bioleaching of gold and copper from waste mobile phone PCBs by using a cyanogenic bacterium. *Minerals Engineering*, 24(11): 1219–1222.

Chiang, H., Lin, K., Lai, M., Chen, T. & Ma, S. 2007. Pyrolysis characteristics of integrated circuit boards at various particle sizes and temperatures. *Journal of Hazardous Materials*, 149(1): 151–159.

Crundwell, F.K. & Godorr, S.A. 1997. A mathematical model of the leaching of gold in cyanide solutions. *Hydrometallurgy*, 44(1–2): 147–162.

Crundwell, F.K., Du Preez, N. & Lloyd, J.M. 2013. Dynamics of particle-size distributions in continuous leaching reactors and autoclaves. *Hydrometallurgy*, 133: 44–50.

Cui, H. & Anderson, C.G. 2016. Literature review of hydrometallurgical recycling of printed circuit boards (PCBs). *Journal of Advanced Chemical Engineering*, 6(1): 142–153.

Cui, J. & Forssberg, E. 2003. Mechanical recycling of waste electric and electronic equipment: a review. *Journal of Hazardous Materials*, 99(3): 243–263.

Cui, J. & Zhang, L. 2008. Metallurgical recovery of metals from electronic waste: A review. *Journal of Hazardous Materials*, 158(2): 228–256.

Dalrymple, I., Wright, N., Kellner, R., Bains, N., Geraghty, K., Goosey, M. & Lightfoot, L. 2007. An integrated approach to electronic waste (WEEE) recycling. *Circuit World*, 33(2): 52–58.

DeCoursey, W.J. 2003. *Statistics and probability for engineering applications with Microsoft Excel*. Woburn, MA: Elsevier.

Didyk-Mucha, A., Pawlowska, A. & Sadowski, Z. 2016. Application of the shrinking core model for dissolution of serpentinite in an acid solution. In *E3S Web of Conferences*. 1035.

Ding, D.-X., Fu, H.-Y., Ye, Y.-J., Hu, N., Li, G.-Y., Song, J.-B. & Wang, Y.-D. 2013. A fractal kinetic model for heap leaching of uranium ore with fractal dimension of varied particle size distribution. *Hydrometallurgy*, 136: 85–92.

Dönmez, B., Sevim, F. & Colak, S. 2001. A study on recovery of gold from decopperized anode slime. *Chemical Engineering & Technology*, 24(1): 91–95.

Dorin, R. & Woods, R. 1991. Determination of leaching rates of precious metals by electrochemical techniques. *Journal of Applied Electrochemistry*, 21(5): 419–424.

Ecroignard, L. 2006. *E-waste Legislation in South Africa*. EngineerIT. www.ee.co.za/wp-content/uploads/legacy/E-waste legislation.pdf.

Ficeriová, J., Baláž, P. & Gock, E. 2011. Leaching of gold, silver and accompanying metals from circuit boards (PCBs) waste. *Acta Montanistica Slovaca*, 16(2): 128–131.

Gámez, S., Garcés, K., de la Torre, E. & Guevara, A. 2019. Precious metals recovery from waste printed circuit boards using thiosulfate leaching and ion exchange resin. *Hydrometallurgy*, 186: 1–11.

Garg, H., Nagar, N., Ellamparuthy, G., Angadi, S.I. & Gahan, C.S. 2019. Bench scale microbial catalysed leaching of mobile phone PCBs with an increasing pulp density. *Heliyon*, 5(12): e02883.

Gbor, P.K., Ahmed, I.B. & Jia, C.Q. 2000. Behaviour of Co and Ni during aqueous sulphur dioxide leaching of nickel smelter slag. *Hydrometallurgy*, 57(1): 13–22.

Gbor, P.K. & Jia, C.Q. 2004. Critical evaluation of coupling particle size distribution with the shrinking core model. *Chemical Engineering Science*, 59(10): 1979–1987.

Gönen, N., Körpe, E., Yildirim, M.E. & Selengil, U. 2007. Leaching and CIL processes in gold recovery from refractory ore with thiourea solutions. *Minerals Engineering*, 20(6): 559–565.

Grosse, A.C., Dicinoski, G.W., Shaw, M.J. & Haddad, P.R. 2003. Leaching and recovery of gold using ammoniacal thiosulfate leach liquors (a review). *Hydrometallurgy*, 69(1–3): 1–21.

Guerra, I. 2010. Peru: toxic waste polluting Opamayo river may reach the Amazon. *Livinginperu.com*. https://www.livinginperu.com/news-12563-environmentnature-peru-toxic-waste-polluting-opamayo-river-may-reach-the-amazon/ 29 March 2018.

Guo, J., Zhang, R. & Xu, Z. 2015. PBDEs emission from waste printed wiring boards during thermal process. *Environmental Science & Technology*, 49(5): 2716–2723.

Guo, X., Liu, J., Qin, H., Liu, Y., Tian, Q. & Li, D. 2015. Recovery of metal values from waste printed circuit boards using an alkali fusion-leaching-separation process. *Hydrometallurgy*, 156: 199–205.

Gupta, C.K. 2003. *Chemical metallurgy: principles and practice*. Weinheim: Wiley-VCH Verlag GmbH & Co. KGaA.

Guzman, L., Yapu, W., Chimenos, J.M., Viladevall, M. & Espiell, F. 1994. Relations between the size distribution of a gold particle system and the leaching curve in cyanide solutions. *Hydrometallurgy*, 36(2): 187–199.

Ha, V.H., Lee, J., Huynh, T.H., Jeong, J. & Pandey, B.D. 2014. Optimizing the thiosulfate leaching of gold from printed circuit boards of discarded mobile phone. *Hydrometallurgy*, 149: 118–126.

Ha, V.H., Lee, J., Jeong, J., Hai, H.T. & Jha, M.K. 2010. Thiosulfate leaching of gold from waste mobile phones. *Journal of Hazardous Materials*, 178(1): 1115–1119.

Habashi, F. 1993. *A textbook of hydrometallurgy*. Quebec City: Métallurgie Extractive Québec.

Hageluken, C. 2006. Improving metal returns and eco-efficiency in electronics recycling-a holistic approach for interface optimisation between pre-processing and integrated metals smelting and refining. In *Electronics and the Environment, 2006. Proceedings of the 2006 IEEE International Symposium on*. 218–223.

Hanafi, J., Jobiliong, E., Christiani, A., Soenarta, D.C., Kurniawan, J. & Irawan, J. 2012. Material recovery and characterization of PCB from electronic waste. *Procedia - Social and Behavioral Sciences*, 57: 331–338.

Herbst, J.A. 1979. Rate processes in multiparticle metallurgical systems. In *Rate processes of extractive metallurgy*. Springer: 53–112.

Hilson, G. & Monhemius, A.J. 2006. Alternatives to cyanide in the gold mining industry: what prospects for the future? *Journal of Cleaner production*, 14(12): 1158–1167.

Holland, L. 2015. *The dangerous path toward mining law reform in Honduras*. Washington, D.C.

http://www.coha.org/wp-content/uploads/2015/12/The-Dangerous-Path-Toward-Mining-Law-Reform-in-Honduras.

Hung, H. V., Hai, H.T., Nga, N.T., Lee, J. & Jeong, J. 2011. Study on effect of temperature on gold leaching from electronic scraps using thiosulphate with copper (II) catalyst in ammonia media. *Journal of Science and Technology*, (82A).

Ilyas, S., Anwar, M.A., Niazi, S.B. & Ghauri, M.A. 2007. Bioleaching of metals from electronic scrap by moderately thermophilic acidophilic bacteria. *Hydrometallurgy*, 88(1–4): 180–188.

Isildar, A., Rene, E.R., Hullebusch, E.D. van & Lens, P.N.L. 2017. Two-step leaching of valuable metals from discarded printed circuit boards, and process optimization using response surface methodology. *Advances in Recycling & Waste Management*, 2(2).

Işıldar, A., van de Vossenberg, J., Rene, E.R., van Hullebusch, E.D. & Lens, P.N.L. 2016. Two-step bioleaching of copper and gold from discarded printed circuit boards (PCB). *Waste Management*, 57: 149–157.

Johnson, D.B. 2014. Biomining - biotechnologies for extracting and recovering metals from ores and waste materials. *Current Opinion in Biotechnology*, 30: 24–31.

Kacham, A.R. & Suri, A.K. 2014. Application of a topochemical reaction model to predict leaching behavior of high carbonate uranium ores in alkaline solutions: An experimental case study. *Hydrometallurgy*, 141: 67–75.

Kasper, A.C., Berselli, G.B.T., Freitas, B.D., Tenório, J.A.S., Bernardes, A.M. & Veit, H.M. 2011. Printed wiring boards for mobile phones: characterization and recycling of copper. *Waste Management*, 31(12): 2536–2545.

Kasper, A.C. & Veit, H.M. 2018. Gold Recovery from Printed Circuit Boards of Mobile Phones Scraps Using a Leaching Solution Alternative to Cyanide. *Brazilian Journal of Chemical Engineering*, 35(3): 931–942.

Kasper, A.C. & Veit, H.M. 2015. Leaching of gold from printed circuit boards scrap of mobile phones. In A. Jha, ed. *Energy Technology 2015*. Cham: Springer: 243–249.

Khaliq, A., Rhamdhani, M., Brooks, G. & Masood, S. 2014. Metal extraction processes for electronic waste and existing industrial routes: a review and australian perspective. *Resources*, 3(1): 152–179.

Khezri, M., Rezai, B., Abdollahzadeh, A.A., Molaeinasab, M., Wilson, B.P. & Lundström, M. 2020. Glycine leaching of Sarcheshmeh chalcopyrite concentrate at high pulp densities in a stirred tank reactor. *Minerals Engineering*, 157: 106555.

Kim, B.-S., Lee, J.-C., Jeong, J., Yang, D.-H., Shin, D. & Lee, K.-I. 2013. A Novel Process for Extracting Precious Metals from Spent Mobile Phone PCBs and Automobile Catalysts. *Materials Transactions*: M2013051.

Kim, Y., Seo, H. & Roh, Y. 2018. Metal recovery from the mobile phone waste by chemical and biological treatments. *Minerals*, 8(1): 8.

Lawhon, M. 2013. Dumping ground or country-in-transition? Discourses of e-waste in South Africa. *Environment and Planning C: Government and Policy*, 31(4): 700–715.

Lehner, T. 2003. E&HS aspects on metal recovery from electronic scrap. In *Electronics and the Environment, 2003. IEEE International Symposium on*. 318–322.

Lehner, T. 1998. Integrated recycling of non-ferrous metals at Boliden Ltd. Ronnskar smelter. In *Electronics and the Environment, 1998. ISEE-1998. Proceedings of the 1998 IEEE International Symposium on*. 42–47.

Levenspiel, O. 1999. *Chemical reaction engineering*. 3rd ed. New York: John Wiley & Sons, Inc.

Li, J., Liang, C. & Ma, C. 2015. Bioleaching of gold from waste printed circuit boards by Chromobacterium violaceum. *Journal of Material Cycles and Waste Management*, 17(3): 529–539.

Li, J. & Miller, J.D. 2007. Reaction kinetics of gold dissolution in acid thiourea solution using ferric sulfate as oxidant. *Hydrometallurgy*, 89(3–4): 279–288.

Liang, G., Tang, J., Liu, W. & Zhou, Q. 2013. Optimizing mixed culture of two acidophiles to improve copper recovery from printed circuit boards (PCBs). *Journal of Hazardous Materials*, 250: 238–245.

Liddell, Kn.C. 2005. Shrinking core models in hydrometallurgy: What students are not being told about the pseudo-steady approximation. *Hydrometallurgy*, 79(1–2): 62–68.

Lu, Y. & Xu, Z. 2016. Precious metals recovery from waste printed circuit boards: a review for current status and perspective. *Resources, Conservation and Recycling*, 113: 28–39.

Marchbank, A.R., Thomas, K.G., Dreisinger, D. & Fleming, C. 1996. Gold recovery from refractory carbonaceous ores by pressure oxidation and thiosulfate leaching. US Patent 5 536 297.

Mark, F.E. & Lehner, T. 2000. Plastics recovery from waste electrical & electronic equipment in non-ferrous metal processes. *Association of Plastics Manufactures in Europe*: 1–23.

Meng, X. & Han, K.N. 1996. The principles and applications of ammonia leaching of metals—a review. *Mineral Processing and Extractive Metullargy Review*, 16(1): 23–61.

MiningWatch. 2006. Groups Call for Action on Cyanide Spills by Multinational Gold Mine in Ghana: International Cyanide Management Institute urged to immediately audit Cyanide Code signatory Golden Star Resources' Bogoso/Prestea mine in Ghana. *MiningWatch*. http://www.miningwatch.ca/news/2006/7/26/groups-call-action-cyanide-spills-multinational-gold-mine-ghana-international-cyanide 29 March 2018.

Molleman, E. & Dreisinger, D. 2002. The treatment of copper-gold ores by ammonium thiosulfate leaching. *Hydrometallurgy*, 66(1–3): 1–21.

Montero, R., Guevara, A. & la Torre, E. 2012. Recovery of gold, silver, copper and niobium from printed circuit boards using leaching column technique. *Journal of Earth Science and Engineering*, 2(10): 6.

Montgomery, D.C. 2017. *Design and analysis of experiments*. 9th ed. Hoboken, NJ: John Wiley & Sons, Inc.

Muir, D.M. & Aylmore, M.G. 2004. Thiosulphate as an alternative to cyanide for gold processing--issues and impediments. *Mineral Processing and Extractive Metallurgy*, 113(1): 2–12.

Natarajan, K.A. 2018. *Biotechnology of metals: principles, recovery methods and environmental concerns*. Elsevier.

Niu, X. & Li, Y. 2007. Treatment of waste printed wire boards in electronic waste for safe disposal. *Journal of Hazardous Materials*, 145(3): 410–416.

Nosrati, A., Quast, K., Xu, D., Skinner, W., Robinson, D.J. & Addai-Mensah, J. 2014. Agglomeration and column leaching behaviour of nickel laterite ores: effect of ore mineralogy and particle size distribution. *Hydrometallurgy*, 146: 29–39.

Ongondo, F.O., Williams, I.D. & Cherrett, T.J. 2011. How are WEEE doing? A global review of the management of electrical and electronic wastes. *Waste Management*, 31(4): 714–730.

Osibanjo, O. & Nnorom, I.C. 2008. Material flows of mobile phones and accessories in Nigeria: Environmental implications and sound end-of-life management options. *Environmental Impact Assessment Review*, 28(2–3): 198–213.

Othusitse, N. & Muzenda, E. 2015. Predictive Models of Leaching Processes: A Critical Review. In *7th International Conference on Latest Trends In Engineering & Technology (ICLTET'2015)*. 136–141.

Park, H.S. & Kim, Y.J. 2019. A novel process of extracting precious metals from waste printed circuit boards: Utilization of gold concentrate as a fluxing material. *Journal of Hazardous Materials*, 365: 659–664.

Perez, A.E. & Galaviz, H.D. 1987. Method for recovery of precious metals from difficult ores with copper -ammonium thiosulfate.

Prosser, A.P. 1996. Review of uncertainty in the collection and interpretation of leaching data. *Hydrometallurgy*, 41(2–3): 119–153.

Pryor, W.A. 1960. The kinetics of the disproportionation of sodium thiosulfate to sodium sulfide and sulfate. *Journal of the American Chemical Society*, 82(18): 4794–4797.

Puckett, J. & Smith, T. 2002. *Exporting Harm: the high-tech trashing of Asia the Basel Network*. Seattle: Silicon Valley Toxics Coalition.

Pyper, R.A. & Hendrix, J.L. 1981. Extraction of gold from finely disseminated gold ores by use of acidic thiourea solution. *Extraction Metallurgy'81*: 57–75.

Quinet, P., Proost, J. & Van Lierde, A. 2005. Recovery of precious metals from electronic scrap by hydrometallurgical processing routes. *Mining, Metallurgy & Exploration*, 22(1): 17–22.

Rath, R.K., Hiroyoshi, N., Tsunekawa, M. & Hirajima, T. 2003. Ammoniacal thiosulphate leaching of gold ore. *EJMP & EP (European Journal of Mineral Processing and Environmental Protection)*, 3(3): 344–352.

Rizki, I.N., Tanaka, Y. & Okibe, N. 2019. Thiourea bioleaching for gold recycling from e-waste. *Waste Management*, 84: 158–165.

Robinson, B.H. 2009. E-waste: an assessment of global production and environmental impacts. *Science of the Total Environment*, 408(2): 183–191.

Rohwerder, T., Gehrke, T., Kinzler, K. & Sand, W. 2003. Bioleaching review part A: Progress in bioleaching: fundamentals and mechanisms of bacterial metal sulfide oxidation. *Applied Microbiology and Biotechnology*, 63(3): 239–248.

Ruan, J., Zhu, X., Qian, Y. & Hu, J. 2014. A new strain for recovering precious metals from waste printed circuit boards. *Waste management*, 34(5): 901–907.

Safari, V., Arzpeyma, G., Rashchi, F. & Mostoufi, N. 2009. A shrinking particle-shrinking core model for leaching of a zinc ore containing silica. *International Journal of Mineral Processing*, 93(1): 79–83.

Schluep, M., Hagelueken, C., Kuehr, R., Magalini, F., Mauer, C., Meskers, C., Mueller, E. & Wang, F. 2009. *Recycling from e-waste to resources, Final Report*. United Nations Environment Program, United Nations University.

Sheng, P.P. & Etsell, T.H. 2007. Recovery of gold from computer circuit board scrap using aqua regia. *Waste Management & Research*, 25(4): 380–383.

Shinkuma, T. & Huong, N.T.M. 2009. The flow of E-waste material in the Asian region and a reconsideration of international trade policies on E-waste. *Environmental Impact Assessment Review*, 29(1): 25–31.

Shuey, S.A. & Taylor, P. 2005. Review of pyrometallurgical treatment of electronic scrap. *Mining Engineering*, 57(4): 67–70.

Skoog, D.A., Holler, F.J., West, D.M. & Crouch, S.R. 2013. *Fundamentals of Analytical Chemistry*. 9th ed. Belmont, CA: Cengage Learning.

Smith, C.W. & Hitchen, A. 1976. Aqueous solution chemistry of polythionates and thiosulfate: a review of formation and degradation pathways. CANMET. *CANMET Mineral Sciences Laboratories Report MRP/MSL*: 76–223.

Sum, E.Y.L. 1991. The recovery of metals from electronic scrap. *JOM*, 43(4): 53–61.

Syed, S. 2012. Recovery of gold from secondary sources - a review. *Hydrometallurgy*, 115: 30–51.

Szałatkiewicz, J. 2014. Metals content in printed circuit board waste. *Polish Journal of Environmental Studies*, 23(6): 2365–2369.

Tripathi, A., Kumar, M., C. Sau, D., Agrawal, A., Chakravarty, S. & R. Mankhand, T. 2012. Leaching of gold from the waste mobile phone printed circuit boards (PCBs) with ammonium thiosulphate. *International Journal of Metallurgical Engineering*, 1(2): 17–21.

Tuncuk, A., Stazi, V., Akcil, A., Yazici, E.Y. & Deveci, H. 2012. Aqueous metal recovery techniques from e-scrap: hydrometallurgy in recycling. *Minerals Engineering*, 25(1): 28–37.

Valix, M. 2017. Bioleaching of Electronic Waste: Milestones and Challenges. In *Current Developments in Biotechnology and Bioengineering*. Elsevier: 407–442.

Vats, M.C. & Singh, S.K. 2015. Assessment of gold and silver in assorted mobile phone printed circuit boards (PCBs). *Waste Management*, 45: 280–288.

Veglio, F., Quaresima, R., Fornari, P. & Ubaldini, S. 2003. Recovery of valuable metals from electronic and galvanic industrial wastes by leaching and electrowinning. *Waste Management*, 23(3): 245–252.

Veglio, F., Trifoni, M., Pagnanelli, F. & Toro, L. 2001. Shrinking core model with variable activation energy: a kinetic model of manganiferous ore leaching with sulphuric acid and lactose. *Hydrometallurgy*, 60(2): 167–179.

Veit, H.M., Bernardes, A.M., Ferreira, J.Z., Tenório, J.A.S. & de Fraga Malfatti, C. 2006. Recovery of copper from printed circuit boards scraps by mechanical processing and electrometallurgy. *Journal of Hazardous Materials*, 137(3): 1704–1709.

Velardo, A., Giona, M., Adrover, A., Pagnanelli, F. & Toro, L. 2002. Two-layer shrinking-core model: parameter estimation for the reaction order in leaching processes. *Chemical Engineering Journal*, 90(3): 231–240.

Veldhuizen, H. & Sippel, B. 1994. Mining discarded electronics. *Industry and Environment*, 17(3): 7–11.

Wang, J. & Xu, Z. 2015. Disposing and recycling waste printed circuit boards: Disconnecting, resource recovery, and pollution control. *Environmental Science & Technology*, 49(2): 721–733.

Wang, X.H. 1992. Thermodynamic Equilibrium Calculations on Au/Ag-Lixiviant Systems Relevant to Gold Extraction from Complex Ores. In *Proceeding of the Third International Symposium on Electrochemistry in Mineral and Metal Processing III*. 452–477.

Wei, L.I.U., Tang, M.-T., Tang, C.-B., Jing, H.E., Yang, S.-H. & Yang, J.-G. 2010. Dissolution kinetics of low grade complex copper ore in ammonia-ammonium chloride solution. *Transactions of Nonferrous Metals Society of China*, 20(5): 910–917.

Widmer, R. & Lombard, R. 2005. *e-Waste assessment in South Africa, a case study of the*

Gauteng province.

Xia, C. & Yen, W.T. 2005. Iron sulfide minerals in thiosulfate-gold leaching: some problems and solutions. In *First International Symposium, Treatment of Gold Ores, 44th Annual Conference of Metallurgists of CIM, Calgary, Alberta, Canada, August*. 21–24.

Xiang, P., Zhang, Y. & Liu, Q. 2018. Gold Leaching from Printed circuit Board Scrap with Thiosulfate. In *IOP Conference Series: Materials Science and Engineering*. 22001.

Xiang, Y., Wu, P., Zhu, N., Zhang, T., Liu, W., Wu, J. & Li, P. 2010. Bioleaching of copper from waste printed circuit boards by bacterial consortium enriched from acid mine drainage. *Journal of Hazardous Materials*, 184(1–3): 812–818.

Xiu, F.-R., Qi, Y. & Zhang, F.-S. 2015. Leaching of Au, Ag, and Pd from waste printed circuit boards of mobile phone by iodide lixiviant after supercritical water pre-treatment. *Waste Management*, 41: 134–141.

Zhang, Y., Liu, S., Xie, H., Zeng, X. & Li, J. 2012. Current status on leaching precious metals from waste printed circuit boards. *Procedia Environmental Sciences*, 16: 560–568.

Zipperian, D., Raghavan, S. & Wilson, J. 1988. Gold and silver extraction by ammoniacal thiosulfate leaching from a rhyolite ore. *Hydrometallurgy*, 19(3): 361–375.

Zulkifli, N.F.M., Jaibee, S., Burhan, M.H., Mohamad, F., Ismail, A.E., Kiong, S.C., Ahmed, Z., Yokoyama, S. & Nor, N.H.M. 2016. Feasibility study of PCB mobiles phones and recycling through manual dismantling and hydrometallurgical method. *ARPN Journal of Engineering and Applied Sciences*, 11(12): 7401–7405.

APPENDICES

APPENDIX A

PARTICLE SIZE DISTRIBUTION

APPENDIX A : Particle Size Distribution

Table A-1: Particle size distribution on frequency basis

Particle Size (μm)	Frequency Mass Fraction			
	PSD 1	PSD 2	PSD 3	PSD 4
0 - 124	0.121	0.133	0.144	0.166
125 - 299	0.182	0.214	0.263	0.290
300 - 599	0.202	0.245	0.258	0.238
600 - 1179	0.222	0.209	0.201	0.166
1180 - 1350	0.273	0.199	0.134	0.140

Table A-2: Particle size distribution on cumulative basis

Particle Size (μm)	Cumulative Undersize Mass Fraction			
	PSD 1	PSD 2	PSD 3	PSD 4
124	0.121	0.133	0.144	0.166
299	0.303	0.347	0.407	0.456
599	0.505	0.592	0.665	0.694
1179	0.727	0.801	0.866	0.860
1350	1.000	1.000	1.000	1.000
D50	592	487	407	354

Table A-3: PSD parameters and central values determined from the Gates-Gaudin-Schuhmann (GGS) model

		Gates-Gaudin-Schuhmann (GGS) Model					
PSD	Actual D_{50} (μm)	m	D_{max} (μm)	R^2	D_{50} (μm)	Mean μ (μm)	Covariance CV
PSD 1	592	0.8246	1456	0.9833	630	658	0.1940
PSD 2	487	0.8004	1333	0.9762	563	593	0.1983
PSD 3	407	0.7694	1236	0.9577	507	537	0.2041
PSD 4	354	0.7046	1235	0.9442	469	510	0.2169

Table A-4: PSD parameters and central values determined from the Rosin-Rammler (RR) model

		Rosin-Rammler (RR) Model					
PSD	**Actual D_{50} (μm)**	**m**	**L (μm)**	**R^2**	**D_{50} (μm)**	**Mean μ (μm)**	**Covariance CV**
PSD 1	592	1.3856	611	0.8588	482	558	0.3088
PSD 2	487	1.3837	551	0.8968	438	503	0.3084
PSD 3	407	1.3772	497	0.9277	396	454	0.3070
PSD 4	354	1.3010	469	0.9161	367	433	0.2879

Table A-5: Fitting of GGS and RR models to PSD 1 data

PSD 1							
Particle Size D (μm)	**Cumulative Mass Fraction F(D)**	**GGS Model**			**RR Model**		
		log D	**log F(D)**	**Predicted F(D)**	**ln D**	**ln {- ln [1 - F(D)]}**	**Predicted F(D)**
124	0.121	2.093	-0.916	0.131	4.820	-2.046	0.104
299	0.303	2.476	-0.519	0.271	5.700	-1.019	0.310
599	0.505	2.777	-0.297	0.481	6.395	-0.352	0.622
1179	0.727	3.072	-0.138	0.840	7.072	0.262	0.917
1350	1.000	3.130	0.000	0.940	7.208	1.933	0.950

Table A-6: Fitting of GGS and RR models to PSD 2 data

PSD 2							
Particle Size D (μm)	**Cumulative Mass Fraction F(D)**	**GGS Model**			**RR Model**		
		log D	**log F(D)**	**Predicted F(D)**	**ln D**	**ln {- ln [1 - F(D)]}**	**Predicted F(D)**
124	0.133	2.093	-0.877	0.149	4.820	-1.950	0.119
299	0.347	2.476	-0.460	0.302	5.700	-0.853	0.349
599	0.592	2.777	-0.228	0.527	6.395	-0.110	0.675
1179	0.801	3.072	-0.096	0.906	7.072	0.479	0.943
1350	1.000	3.130	0.000	1.010	7.208	1.933	0.968

Table A-7: Fitting of GGS and RR models to PSD 3 data

PSD 3							
Particle Size D (μm)	Cumulative Mass Fraction F(D)	GGS Model			RR Model		
		log D	log F(D)	Predicted F(D)	ln D	ln {- ln [1 - F(D)]}	Predicted F(D)
124	0.144	2.093	-0.841	0.171	4.820	-1.859	0.137
299	0.407	2.476	-0.390	0.336	5.700	-0.648	0.392
599	0.665	2.777	-0.177	0.573	6.395	0.089	0.726
1179	0.866	3.072	-0.062	0.965	7.072	0.698	0.963
1350	1.000	3.130	0.000	1.070	7.208	1.933	0.981

Table A-8: Fitting of GGS and RR models to PSD 4 data

PSD 4							
Particle Size D (μm)	Cumulative Mass Fraction F(D)	GGS Model			RR Model		
		log D	log F(D)	Predicted F(D)	ln D	ln {- ln [1 - F(D)]}	Predicted F(D)
124	0.166	2.093	-0.780	0.198	4.820	-1.708	0.162
299	0.456	2.476	-0.341	0.368	5.700	-0.496	0.427
599	0.694	2.777	-0.158	0.601	6.395	0.170	0.747
1179	0.860	3.072	-0.065	0.968	7.072	0.676	0.964
1350	1.000	3.130	0.000	1.065	7.208	1.933	0.981

APPENDIX B

AMMONIUM THIOSULPHATE LEACHING

APPENDIX B : Ammonium Thiosulphate Leaching

B.1 Gold Extraction

Table B-1: Gold concentration (mg/L) of pregnant thiosulphate leach solutions

Conditions		Reaction Time (h)						
PD (g/L)	PSD	0	0.5	1	1.5	2	2.5	3
40	1	0	5.44	5.45	5.47	4.59	4.38	3.75
40	2	0	3.21	4.78	5.90	6.38	5.36	5.98
40	3	0	5.34	5.34	5.70	5.74	4.58	6.20
40	4	0	3.28	4.35	6.06	6.70	6.76	6.81
80	1	0	3.24	5.46	5.62	6.00	6.31	4.78
80	2	0	5.24	6.30	7.16	4.96	7.70	5.94
80	3	0	4.00	2.29	3.78	4.16	5.14	5.58
80	4	0	5.92	6.84	4.89	4.93	5.35	5.22
120	1	0	6.13	6.26	6.22	6.58	6.76	6.11
120	2	0	6.69	6.95	6.53	7.21	7.13	7.41
120	3	0	7.67	8.12	7.49	7.55	8.11	7.67
120	4	0	7.63	8.82	8.66	8.10	8.37	7.99

Table B-2: Gold conversion by thiosulphate leaching

Conditions		Reaction Time (h)						
PD (g/L)	PSD	0	0.5	1	1.5	2	2.5	3
40	1	0	0.79	0.79	0.79	0.67	0.64	0.54
40	2	0	0.47	0.69	0.86	0.93	0.78	0.87
40	3	0	0.78	0.78	0.83	0.83	0.67	0.90
40	4	0	0.48	0.63	0.88	0.97	0.98	0.99
80	1	0	0.24	0.40	0.41	0.44	0.46	0.35
80	2	0	0.38	0.46	0.52	0.36	0.56	0.43
80	3	0	0.29	0.17	0.27	0.30	0.37	0.41
80	4	0	0.43	0.50	0.36	0.36	0.39	0.38
120	1	0	0.30	0.30	0.30	0.32	0.33	0.30
120	2	0	0.32	0.34	0.32	0.35	0.35	0.36
120	3	0	0.37	0.39	0.36	0.37	0.39	0.37
120	4	0	0.37	0.43	0.42	0.39	0.41	0.39

B.2 Statistical Analysis - ANOVA

Table B-3: Response means – Au conversion

PD	PSD			
	PSD 1	PSD 2	PSD 3	PSD 4
40	0.60	0.66	0.68	0.71
80	0.33	0.39	0.26	0.34
120	0.26	0.29	0.32	0.34

PD: Pulp Density

PSD: Particle Size Distribution

Table B-4: Descriptive statistics

Source of Variation	*Levels*	*Count*	*Sum*	*Average*	*Variance*
Pulp Density	40	4	2.64833	0.66208	0.00191
	80	4	1.31651	0.32913	0.00284
	120	4	1.21908	0.30477	0.00124
PSD	PSD 1	3	1.19313	0.39771	0.03280
	PSD 2	3	1.33370	0.44457	0.03600
	PSD 3	3	1.26474	0.42158	0.05232
	PSD 4	3	1.39235	0.46412	0.04357

Table B-5: Anova: two-factor without replication

Source of Variation	*Sum of Squares (SS)*	*df*	*Mean Square (MS)*	*F*	*P-value*	*F crit*
Pulp Density	0.318828	2	0.159414	90.6428	0.00003	5.143253
PSD	0.007421	3	0.002474	1.406595	0.32955	4.757063
Within (Error)	0.010552	6	0.001759			
Total	0.336802	11				

APPENDIX C

SHRINKING-CORE MODEL AND RATE-LIMITING MECHANISM

APPENDIX C : Shrinking-Core Model and Rate-Limiting Mechanism

C.1 Fitting of SCM to Leaching Data at High Pulp Densities

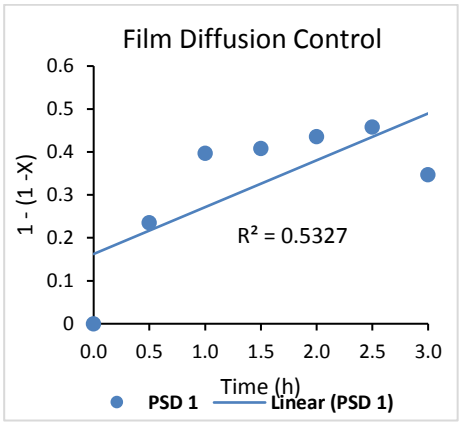

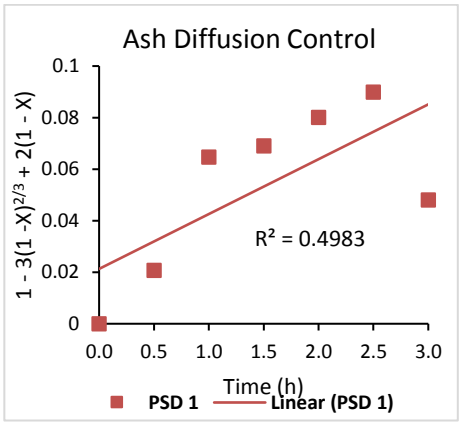

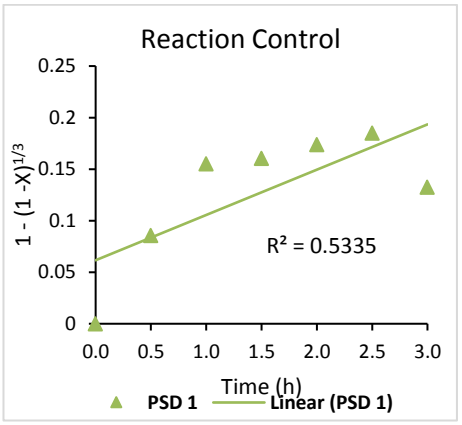

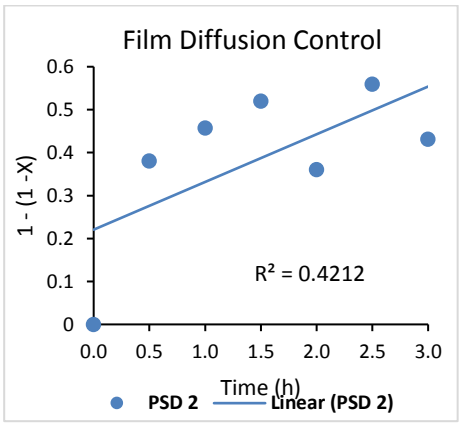

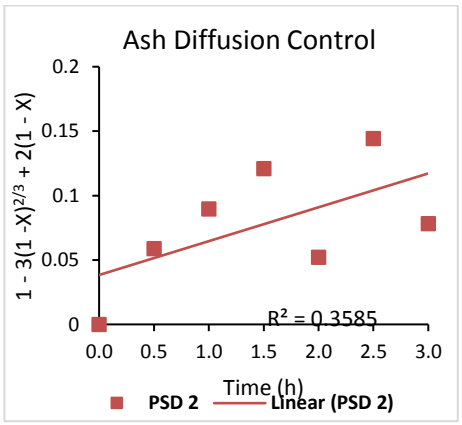

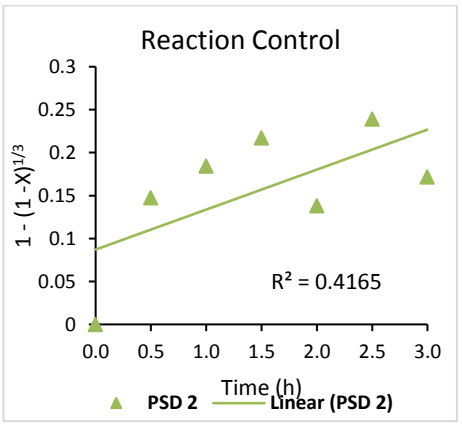

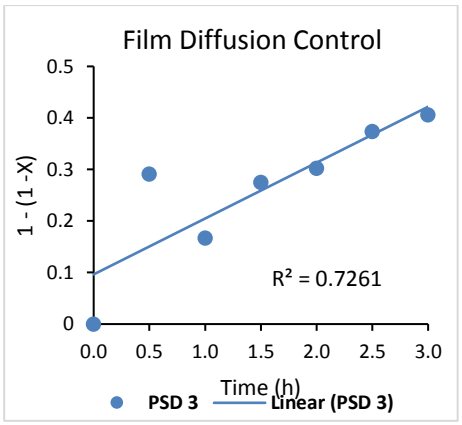

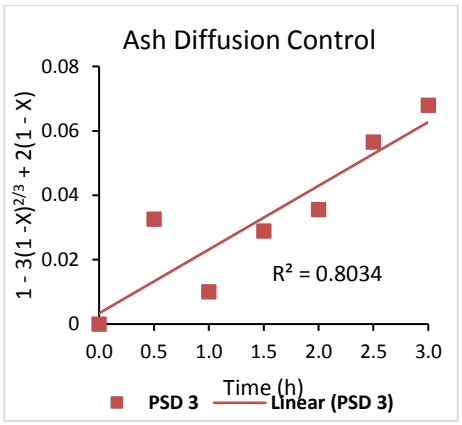

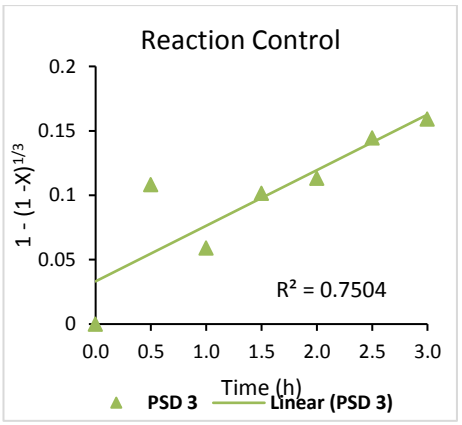

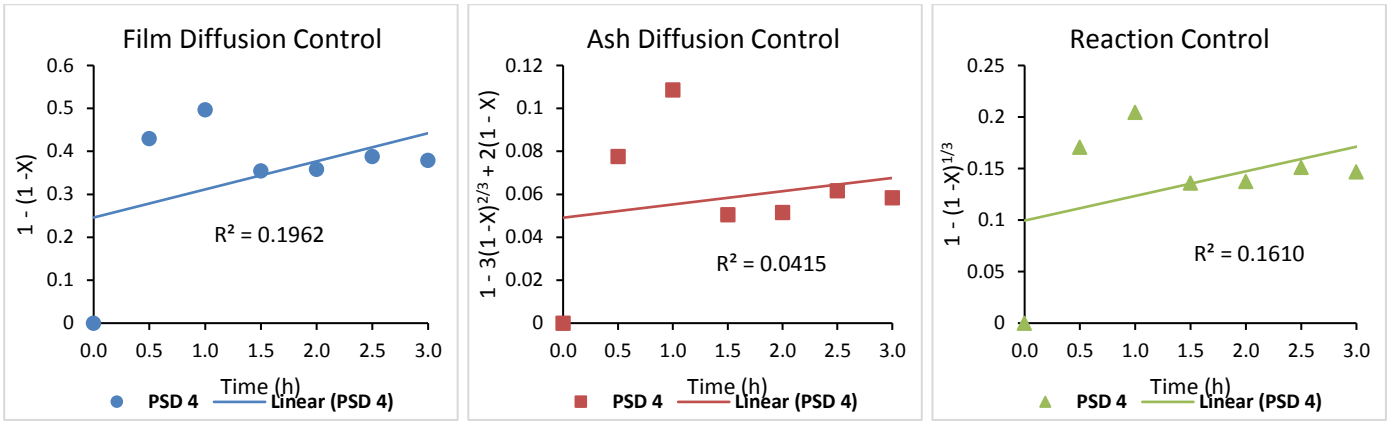

Figure C-1: Fitting of SCM to leaching experimental data for 80 g/L pulp density

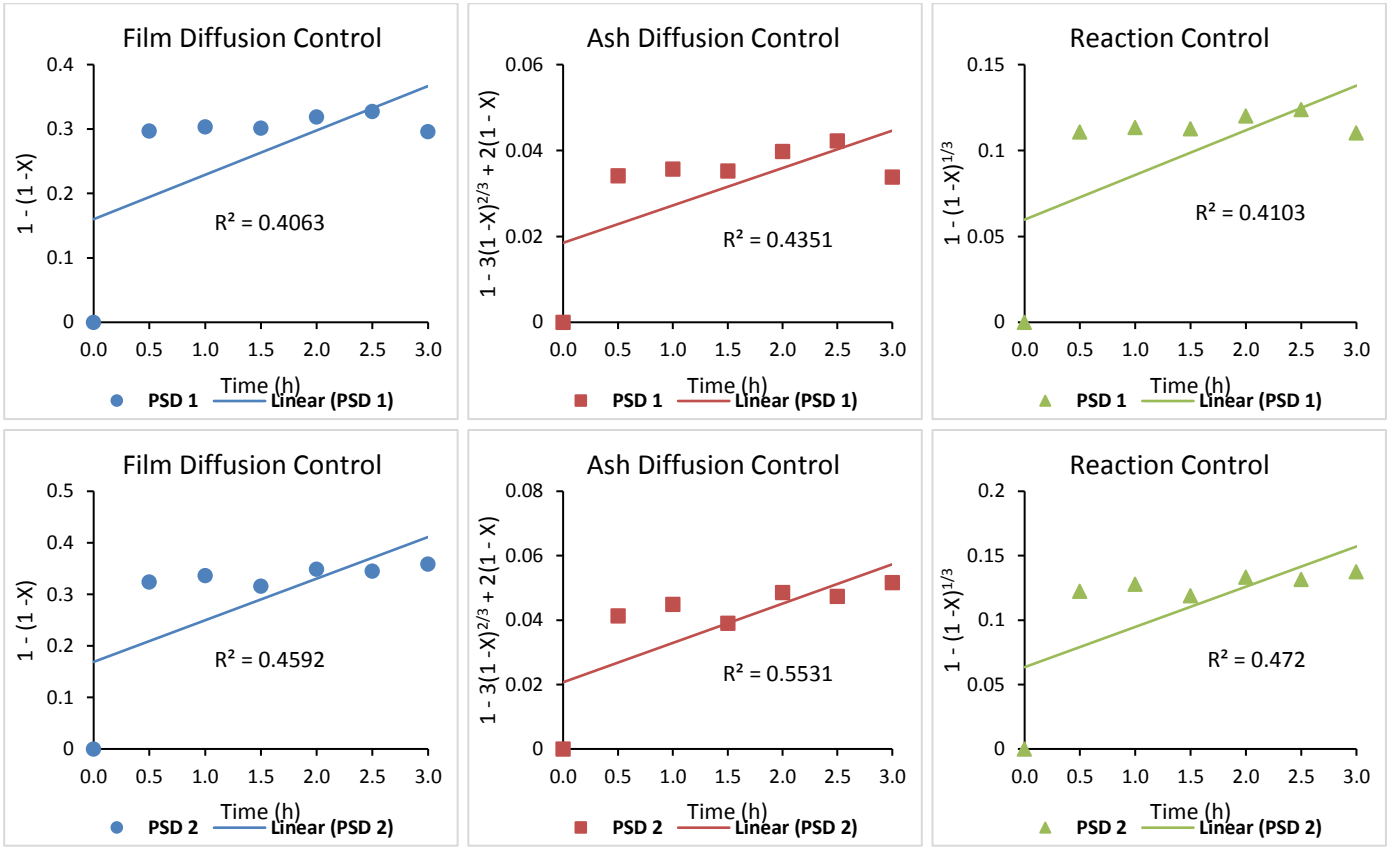

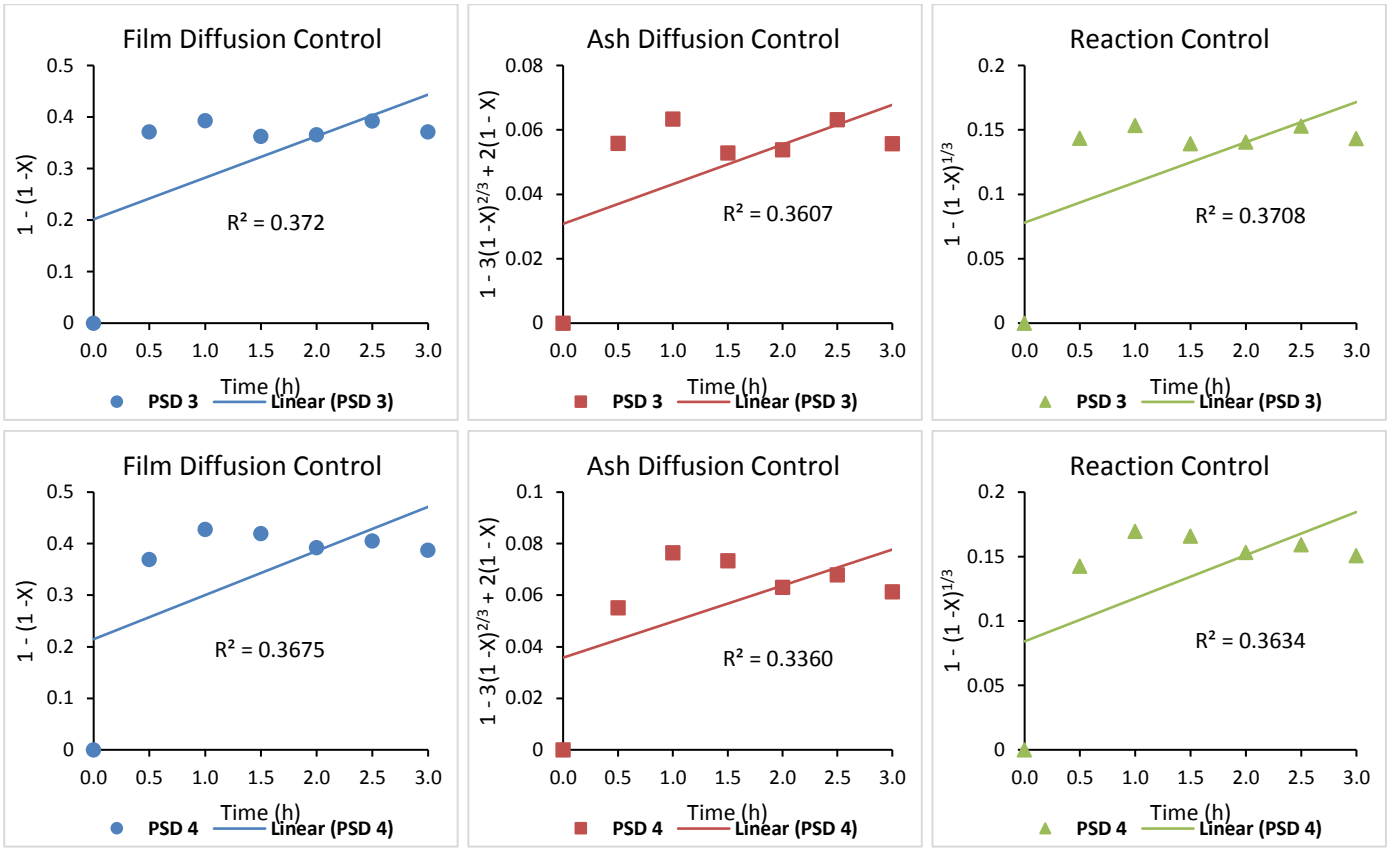

Figure C-2: Fitting of SCM to leaching experimental data for 120 g/L pulp density

C.2 SCM-generated and Experimental Data

Table C-1: SCM-generated data and experimental data – 40 g/L PD & PSD 1

Time (h)	X	FDC $1-(1-X)$	ADC $1-3(1-X)^{2/3}+2(1-X)$	RC $1-(1-X)^{1/3}$
0.0	0	0	0	0
0.5	0.7907	0.7907	0.3610	0.4063
1.0	0.7917	0.7917	0.3624	0.4072
1.5	0.7946	0.7946	0.3664	0.4100
2.0	0.6676	0.6676	0.2253	0.3073
2.5	0.6366	0.6366	0.1991	0.2864
3.0	0.5446	0.5446	0.1350	0.2306

FDC: Liquid film diffusion control

ADC: Ash layer diffusion control

RC: Chemical reaction control

Table C-2: SCM-generated data and experimental data – 40 g/L PD & PSD 2

Time (h)	X	FDC $1-(1-X)$	ADC $1-3(1-X)^{2/3}+2(1-X)$	RC $1-(1-X)^{1/3}$
0.0	0.00	0	0	0
0.5	0.4666	0.4666	0.0937	0.1890
1.0	0.6948	0.6948	0.2505	0.3267
1.5	0.8576	0.8576	0.4666	0.4777
2.0	0.9273	0.9273	0.6229	0.5827
2.5	0.7791	0.7791	0.3455	0.3955
3.0	0.8692	0.8692	0.4885	0.4924

Table C-3: SCM-generated data and experimental data – 40 g/L PD & PSD 3

Time (h)	X	FDC $1-(1-X)$	ADC $1-3(1-X)^{2/3}+2(1-X)$	RC $1-(1-X)^{1/3}$
0.0	0.00	0	0	0
0.5	0.7762	0.7762	0.3417	0.3928
1.0	0.7762	0.7762	0.3417	0.3928
1.5	0.8285	0.8285	0.4169	0.4444
2.0	0.8343	0.8343	0.4264	0.4507
2.5	0.6657	0.6657	0.2236	0.3060
3.0	0.9012	0.9012	0.5564	0.5376

Table C-4: SCM-generated data and experimental data – 40 g/L PD & PSD 4

Time (h)	X	FDC $1-(1-X)$	ADC $1-3(1-X)^{2/3}+2(1-X)$	RC $1-(1-X)^{1/3}$
0.0	0.00	0	0	0
0.5	0.4767	0.4767	0.0985	0.1942
1.0	0.6328	0.6328	0.1960	0.2839
1.5	0.8808	0.8808	0.5118	0.5079
2.0	0.9738	0.9738	0.7879	0.7031
2.5	0.9826	0.9826	0.8331	0.7407
3.0	0.9893	0.9893	0.8760	0.7799

Table C-5: SCM-generated data and experimental data – 80 g/L PD & PSD 1

Time (h)	X	FDC $1-(1-X)$	ADC $1-3(1-X)^{2/3}+2(1-X)$	RC $1-(1-X)^{1/3}$
0.0	0	0	0	0
0.5	0.2355	0.2355	0.0207	0.0856
1.0	0.3968	0.3968	0.0647	0.1551
1.5	0.4084	0.4084	0.0690	0.1605
2.0	0.4360	0.4360	0.0801	0.1738
2.5	0.4583	0.4583	0.0899	0.1848
3.0	0.3474	0.3474	0.0481	0.1326

Table C-6: SCM-generated data and experimental data – 80 g/L PD & PSD 2

Time (h)	X	FDC $1-(1-X)$	ADC $1-3(1-X)^{2/3}+2(1-X)$	RC $1-(1-X)^{1/3}$
0.0	0.00	0	0	0
0.5	0.3808	0.3808	0.0590	0.1477
1.0	0.4578	0.4578	0.0896	0.1846
1.5	0.5203	0.5203	0.1211	0.2172
2.0	0.3605	0.3605	0.0522	0.1384
2.5	0.5596	0.5596	0.1443	0.2392
3.0	0.4317	0.4317	0.0783	0.1717

Table C-7: SCM-generated data and experimental data – 80 g/L PD & PSD 3

Time (h)	X	FDC $1-(1-X)$	ADC $1-3(1-X)^{2/3}+2(1-X)$	RC $1-(1-X)^{1/3}$
0.0	0.00	0	0	0
0.5	0.2907	0.2907	0.0326	0.1082
1.0	0.1667	0.1667	0.0100	0.0590
1.5	0.2747	0.2747	0.0288	0.1015
2.0	0.3023	0.3023	0.0355	0.1131
2.5	0.3735	0.3735	0.0565	0.1443
3.0	0.4055	0.4055	0.0679	0.1592

Table C-8 SCM-generated data and experimental data – 80 g/L PD & PSD 4

Time (h)	X	FDC $1-(1-X)$	ADC $1-3(1-X)^{2/3}+2(1-X)$	RC $1-(1-X)^{1/3}$
0.0	0.00	0	0	0
0.5	0.4302	0.4302	0.0777	0.1710
1.0	0.4971	0.4971	0.1086	0.2048
1.5	0.3551	0.3551	0.0505	0.1360
2.0	0.3585	0.3585	0.0516	0.1376
2.5	0.3886	0.3886	0.0617	0.1512
3.0	0.3794	0.3794	0.0585	0.1470

Table C-9: SCM-generated data and experimental data – 120 g/L PD & PSD 1

Time (h)	X	FDC $1-(1-X)$	ADC $1-3(1-X)^{2/3}+2(1-X)$	RC $1-(1-X)^{1/3}$
0.0	0	0	0	0
0.5	0.2968	0.2968	0.0341	0.1108
1.0	0.3033	0.3033	0.0357	0.1135
1.5	0.3014	0.3014	0.0352	0.1127
2.0	0.3188	0.3188	0.0398	0.1201
2.5	0.3275	0.3275	0.0422	0.1239
3.0	0.2959	0.2959	0.0338	0.1104

Table C-10: SCM-generated data and experimental data – 120 g/L PD & PSD 2

Time (h)	X	FDC $1-(1-X)$	ADC $1-3(1-X)^{2/3}+2(1-X)$	RC $1-(1-X)^{1/3}$
0.0	0.00	0	0	0
0.5	0.3243	0.3243	0.0413	0.1225
1.0	0.3369	0.3369	0.0449	0.1280
1.5	0.3162	0.3162	0.0391	0.1190
2.0	0.3492	0.3492	0.0486	0.1334
2.5	0.3453	0.3453	0.0474	0.1317
3.0	0.3589	0.3589	0.0517	0.1377

Table C-11: SCM-generated data and experimental data – 120 g/L PD & PSD 3

Time (h)	X	FDC $1-(1-X)$	ADC $1-3(1-X)^{2/3}+2(1-X)$	RC $1-(1-X)^{1/3}$
0.0	0.00	0	0	0
0.5	0.3718	0.3718	0.0559	0.1435
1.0	0.3934	0.3934	0.0634	0.1535
1.5	0.3627	0.3627	0.0529	0.1395
2.0	0.3656	0.3656	0.0539	0.1408
2.5	0.3928	0.3928	0.0632	0.1532
3.0	0.3714	0.3714	0.0558	0.1434

Table C-12: SCM-generated data and experimental data – 120 g/L PD & PSD 4

Time (h)	X	FDC $1-(1-X)$	ADC $1-3(1-X)^{2/3}+2(1-X)$	RC $1-(1-X)^{1/3}$
0.0	0.00	0	0	0
0.5	0.3695	0.3695	0.0551	0.1425
1.0	0.4273	0.4273	0.0765	0.1696
1.5	0.4196	0.4196	0.0734	0.1658
2.0	0.3924	0.3924	0.0631	0.1530
2.5	0.4054	0.4054	0.0679	0.1591
3.0	0.3873	0.3873	0.0612	0.1506

APPENDIX D

SAMPLE CALCULATIONS

APPENDIX D : Sample Calculations

D.1 PCB Characterisation

The gold content of PCBs was calculated as follows. 5 g PCB was dissolved in 40 mL aqua regia solution. The final gold concentration of the pregnant leach solution was found to be **21.5 mg/L**. Thus:

$m_T = 5\ g = 5000\ mg\ \ (PCB\ mass)$

$V_T = 40\ mL$

$C_{Au} = 21.5\ mg/L$

$m_{Au} = 21.5\ \frac{mg}{L}\left(\frac{1\ L}{1000\ mL}\right)(40\ mL) = \underline{0.86\ mg\ Au}$

$x_{Au} = \frac{m_{Au}}{m_T} = \frac{0.86\ mg\ Au}{5000\ mg\ Au} = \underline{0.000172}$

$\boxed{\boldsymbol{Au\ Content} = \mathbf{0.0172\ wt\%}}$

$Au\ Content = 0.000172\ \frac{ton\ Au}{ton\ PCB}\left(\frac{10^6\ g\ Au}{1\ ton\ Au}\right)$

$\boxed{\boldsymbol{Au\ Content} = \mathbf{172\ g/ton\ PCB}}$

D.2 Gold Conversion – Sample Calculations for 40 g/L PD & PSD 4

$Pulp\ density = 40\ g/L$

$Reaction\ Volume = 500\ mL = 0.500\ L$

$PCB\ mass = Pulp\ density\ x\ Reaction\ Volume = \left(40\ \frac{g}{L}\right)(0.500\ L) = 20\ g$

Based on the initial gold content (0.0172 wt% Au), the mass gold in 20 g of PCB is:

$m_{Au\ initial} = \frac{0.0172(20)}{100} = \underline{0.00344\ g}$

The gold concentration of the pregnant leach solution after **2 hours** (Table B-1) was **6.70 mg/L**. Thus:

$$m_{Au\ dissolved} = 6.70\ \frac{mg}{L}\left(\frac{1g}{1000\ mg}\right)(0.500\ L) = 0.00335\ g$$

$$Au\ Conversion = \frac{m_{Au\ dissolved}}{m_{Au\ initial}} = \frac{0.00335\ g}{0.00344g} = \boxed{\mathbf{0.97}}$$

D.3 Mathematical Derivation of the Shrinking-Core Model – Reaction Control

In this section, the derivation of the SCM in terms of reaction control is outlined. The remaining SCMs have been derived and discussed extensively by Levenspiel (1999).

Considering the following reaction between a solid A surrounded by a fluid B:

$$A(f) + bB(s) \longrightarrow products \tag{9}$$

When a solid-fluid reaction is chemically controlled, the interaction is independent of the presence of any ash or film layer surrounding the unreacted particle core. The rate of reaction is therefore proportional to the total surface of the unreacted core. The reaction rate for the stoichiometry of reaction (9) is:

$$-\frac{1}{4\pi r_c^2}\frac{dN_B}{dt} = -\frac{b}{4\pi r_c^2}\frac{dN_A}{dt} = bk"C_{Ag} \tag{D-1}$$

Where k" is the first-order rate constant for the surface reaction.

Writing N_B as a function of the unreacted radius r_c and substituting in equation (D-1) gives:

$$-\frac{1}{4\pi r_c^2}\rho_B 4\pi r_c^2\frac{dr_c}{dt} = -\rho_B\frac{dr_c}{dt} = bk"C_{Ag} \tag{D-2}$$

Integrating gives:

$$-\rho_B\int_R^{r_c} dr_c = bk"C_{Ag}\int_0^t dt \tag{D-3}$$

$$\boxed{t = \frac{\rho_b}{bk"C_{Ag}}(R - r_c)} \tag{D-4}$$

Complete conversion corresponds to the disappearance of the unreacted core. Thus, taking the time for total conversion as τ and corresponding unreacted core size $r_c = 0$ gives:

$$\boxed{\tau = \frac{\rho_b R}{bk"C_{Ag}}} \tag{15}$$

The size reduction of the unreacted core or increase in the fractional conversion can be expressed in terms of τ by combining equations (D-4) and (15), giving:

$$\boxed{\frac{t}{\tau} = 1 - \frac{r_c}{R} = 1 - (1 - X_B)^{1/3}} \tag{14}$$